Rochester Institute of Technology
RIT Digital Institutional Repository

Theses

4-2018

Application of Convolutional Neural Network Framework on Generalized Spatial Modulation for Next Generation Wireless Networks

Akram Marseet
am9550@rit.edu

Follow this and additional works at: https://repository.rit.edu/theses

Recommended Citation

Marseet, Akram, "Application of Convolutional Neural Network Framework on Generalized Spatial Modulation for Next Generation Wireless Networks" (2018). Thesis. Rochester Institute of Technology. Accessed from

This Thesis is brought to you for free and open access by the RIT Libraries. For more information, please contact repository@rit.edu.

Application of Convolutional Neural Network Framework on Generalized Spatial Modulation for Next Generation Wireless Networks

by

Akram Marseet

A Thesis Submitted in Partial Fulfillment of the Requirements for the Degree of Master of Science in Electrical Engineering

Supervised by

Dr. Ferat Sahin
Department of Electrical and Microelectronic Engineering
Kate Gleason College of Engineering
Rochester Institute of Technology. Rochester, New York
April 2018

Approved by:

Dr. Ferat Sahin, Professor
Thesis Advisor, Department of Electrical and Microelectronic Engineering

---

Dr. Gill Tsouri, Associate Professor
Committee Member, Department of Electrical and Microelectronic Engineering

---

Dr. Sohail A. Dianat, Professor
Committee Member, Department of Electrical and Microelectronic Engineering

---

Dr. Sohail A. Dianat, Professor
Department Head, Department of Electrical and Microelectronic Engineering

Thesis Release Permission Form

Rochester Institute of Technology
Kate Gleason College of Engineering

Title:

Application of Complex-Valued Neural Network on Generalized Spatial Modulation for Next Generation Wireless Networks

I, Akram Marseet, hereby grant permission to the Wallace Memorial Library to reproduce my thesis in whole or part.

Akram Marseet

Date

Dedication

I dedicate this thesis to my parents, teachers and colleagues.

Acknowledgments

I am greatly thankful to my thesis advisor Dr. Ferat Sahin for his supporting and guiding me during my research. It was great honor and privilege for me to be one of his graduate students, and I will be his PhD student.

I would like to give special thanks to my colleague Tuly Hazbar for her continuous support and encouragement.

I would like to thank my friend Celal Savur for his feedback about my thesis.

I am thankful to my sponsor; the ministry of High education of my home country "Libya."

Abstract

Application of Convolutional Neural Network Framework on Generalized Spatial Modulation for Next Generation Wireless Networks

Akram Marseet

Supervising Professor: Dr. Ferat Sahin

A novel custom auto-encoder Complex Valued Convolutional Neural Network (AE-CV-CNN) model is proposed and implemented using MATLAB for multiple-input-multiple output (MIMO) wireless networks. The proposed model is applied on two different generalized spatial modulation (GSM) schemes: the single symbol generalized spatial modulation $SS-GSM$ and the multiple symbol generalized spatial modulation (MS-GSM). GSM schemes are used with Massive-MIMO to increase both the spectrum efficiency and the energy efficiency. On the other hand, GSM schemes are subjected to high computational complexity at the receiver to detect the transmitted information. High computational complexity slows down the throughput and increases the power consumption at the user terminals. Consequently, reducing both the total spectrum efficiency and energy efficiency. The proposed CNN framework achieves constant complexity reduction of 22.73% for SS-GSM schemes compared to the complexity of its traditional maximum likelihood detector (ML). Also, it gives a complexity reduction of 14.7% for the MS-GSM schemes compared to the complexity of its detector. The performance penalty of the two schemes is at most 0.5 dB. Besides to the proposed custom AE CV-CNN model, a different ML detector′s formula for $(SS-GSM)$ schemes is proposed that achieves the same performance as the traditional

ML detector with a complexity reduction of at least 40% compared to that of the traditional ML detector. In addition, the proposed AE-CV-CNN model is applied to the proposed ML detector,and it gives a complexity reduction of at least 63.6% with a performance penalty of less than 0.5 dB. An interesting result about applying the proposed custom CNN model on the proposed ML detector is that the complexity is reduced as the spatial constellation size is increased which means that the total spectrum efficiency is increased by increasing the spatial constellation size without increasing the computational complexity.

List of Contributions

- Convolutional Neural Network framework for modeling the receiver of wireless MIMO communication system.
- Developing a novel and custom feed forward complex valued convolutional neural network (CV-CNN) for the detection process on wireless MIMO systems.
- Implementation of the joint detection of the spatial and constellation information on generalized spatial modulation schemes based in CNN framework.
- Modeling the estimation of the wireless channel coefficients as the learning process of the weights of the proposed neural network.
- Developing a new maximum likelihood detector for M-ary Phase Shift Modulation schemes (MPSK) with lower computational complexity compared to the traditional maximum likelihood detector.
- Implementing the proposed CNN model with extracted features from the proposed ML detector for further reduction of the computational complexity.
- **Publication: Accepted and presented** (*On print*)

  A. Marseet and F. Sahin, "Application of Complex-Valued Convolutional Neural Network for Next Generation Wireless Networks," 2017 IEEE Western New York Image and Signal Processing Workshop (WNYISPW), Rochester, NY, 2017.

Contents

List of Tables

List of Figures

Chapter 1

Introduction

The demand on wireless communication services is dramatically increasing [1] while the physical resources of wireless networks are limited. The physical resources of wireless communications are the allocated spectrum and the transmission power [2]. The huge demand on cellular wireless services is not only due to the mobile phone services, but also because of machine-to machine communication and the Internet of things (IoT) where there will be billions of devices connected to the Internet [3]. The evolution for next-generation wireless networks is to support the high data rates up to 10 Gbps at lower time delay[4]. Multiple-input multiple-output (MIMO) networks is the key technology of current wireless cellular networks [5] where the term "multiple-input" refers to the use of multiple antennas at the transmitter which are considered as the inputs to the channel, and the term "multiple-output" refers to the use of multiple antennas at the receiver which are considered as the outputs of the channel.

Current wireless networks are called 4G wireless networks which are based on orthogonal frequency division multiplexing (OFDM) for the down link transmission. OFDM is a multi-carrier transmission technique where the allocated bandwidth is subdivided into a set of orthogonal signals with small bandwidths for each sub-carrier to avoid the distortion

due to frequency selective fading channels [6]. Long term evolution LTE is the most spectrum efficient MIMO wireless technology that is able to support data rates up to 1 *Gbps* [7]. However, to catch up the increasing growth on wireless communication services, next generation must be able to support up to 10 *Gbps* [8].

Besides the lack of current wireless MIMO networks to achieve the high speed data communications, another issue is the low energy efficiency [9]. Because of the multiple transmissions on traditional MIMO systems such as vertical Bell Labs layered space time (VBLAST), multiple Radio Frequency (RF) chains including power amplifiers are required at the base station which causes the operating costs of wireless networks [10]. In addition to the low energy efficiency of current MIMO systems, there are other issues such as system′s performance degradation due to the the inter-channel interference (ICI) that is resulted because of the simultaneous transmissions over the same carrier frequencies [11]. Furthermore, precise synchronization between all transmit antennas is mandatory to achieve the maximum spectrum efficiency [12].

The transmission bandwidth is measured in Hz and the transmission energy is measured in joules per bit. The more number of transmitted bits per second per Hz, the more spectrum efficient transmission system. The lower consumed transmission power per bit, the more energy efficient scheme. Spatial modulation is a transmission scheme that depends on both the transmitted signals and the channel characteristics to convey the information [13]. Because of the extra information that are conveyed by the wireless channel without any cost on the bandwidth or the transmitted power, spatial modulation is the most spectrum and energy efficient MIMO scheme. However, the main issue of Spatial Modulation MIMO

systems is the computational complexity at the receiver. This complexity comes due to the joint detection of the spatial and modulation information [14].

In [15] , inspired by the principles of neural Networks, the Wireless MIMO network can be modeled as an auto-encoder convolutional neural network. Since the wireless channel and the receiver noise introduce a distortion to the transmitted signal, the received signal is different from the transmitted signal. In other words, the transmitted information are encoded. To detect the transmitted bits, it is necessary to estimate the channel coefficients to perform the decoding process. The estimation of the transmission channel coefficients is similar to learning weights that the machine learning model is trained to learn these weights.

The purpose of this thesis is to apply the concept of deep learning and especially the concept of auto-encoder convolutional neural network to detect the transmitted information on the high spectrum and energy efficient wireless scheme which is known as generalized Spatial Modulation (GSM). The proposed model of the custom convolutional neural network is used for the joint detection of the spatial and signal constellation information at lower computational complexity compared to the maximum likelihood detector.

Chapter 2

Overview of MIMO Wireless Networks

Current Multiple Input Multiple Output (MIMO) wireless networks are considered as a 2D transmission schemes where the transmitted information are conveyed by the 2D transmitted signal. The transmitted signal is called the modulated signal.

2.1 Modulated Signals

Modulated signal is used for the transmission of digital information. Basically, modulation process involves the change of either amplitude, phase, frequency, or any combination of these parameters of a carrier signal according to the information signals to be transmitted. If the amplitude , phase, or both are changed, the resulted modulated signal is 2D signal. Mathematically, the 2D modulated signal can be expressed as a complex number. A 2D signal is can be constructed from two orthogonal signals $\psi_1(t)$ and $\psi_2(t)$. The $\psi_1(t) - \psi_2(t)$ space is known as the signal constellation where the signal component on the $\psi_1(t)$ dimension is called the in-phase component and the signal component on the $\psi_2(t)$ dimension is called the quadrature phase component. The two most common modulation schemes (also called constellation) are the M-array phase shift keying ($MPSK$) and the M-array amplitude-phase shift keying ($MAPSK$) which is commonly known as ($MQAM$). The letter M represents the size of the signal constellation (It is also called the modulation order).

It represents the number of unique symbols that are used for mapping a certain sequence of information bits with a length of l.

2.1.1 M-arry Phase Shift Keying

In MPSK, the transmitted information are conveyed by the phase of the transmitted modulated signal. MPSK signal has a constant symbol$'s$ power and called constant envelope signal. The MPSK modulated signal $s_m(t)$, $m = 1, 2, ...M$ is given in Eq. 2.1.

$$s_m(t) = \sqrt{E_s}\,[cos(\phi_m)p(t)cos\,(2\pi f_c t) - sin(\phi_m)p(t)sin\,(2\pi f_c t)] \tag{2.1}$$

where E_s is the symbol$'$ energy, ϕ_m is the symbols$'$ phase, f_c is the carrier frequency, and $p(t)$ is the signal of the transmitted symbol. The phase ϕ_m of the m^{th} symbol is given by:

$$\phi_m = \frac{(2m-1)\pi}{M} \tag{2.2}$$

Since the $MPSK$ signal is a 2D signal, equation (5) can be written as:

$$s_m(t) = S_{mI}\psi_1(t) + S_{mQ}\psi_2(t) \tag{2.3}$$

where S_{mI} is the in-phase component given in (8) and S_{mQ} is the quadrature phase component given in Eqs. 2.4 and 2.5.

$$S_{mI} = \sqrt{E_s}cos(\phi_m) \tag{2.4}$$

$$S_{mQ} = \sqrt{E_s}sin(\phi_m) \tag{2.5}$$

The signals $\psi_1(t)$ and ψ_2 are given by:

$$\psi_1(t) = p(t)cos\,(2\pi f_c t) \tag{2.6}$$

$$\psi_2(t) = -p(t)sin\,(2\pi f_c t) \tag{2.7}$$

In MPSK, the modulation spectrum efficiency (l) is related to the modulation order (M) as given in Eq.2.8.

$$l = log_2(M) \tag{2.8}$$

Figure 2.1 shows the signal constellation diagram for the $4PSK$ signals which is also know as $QPSK$.

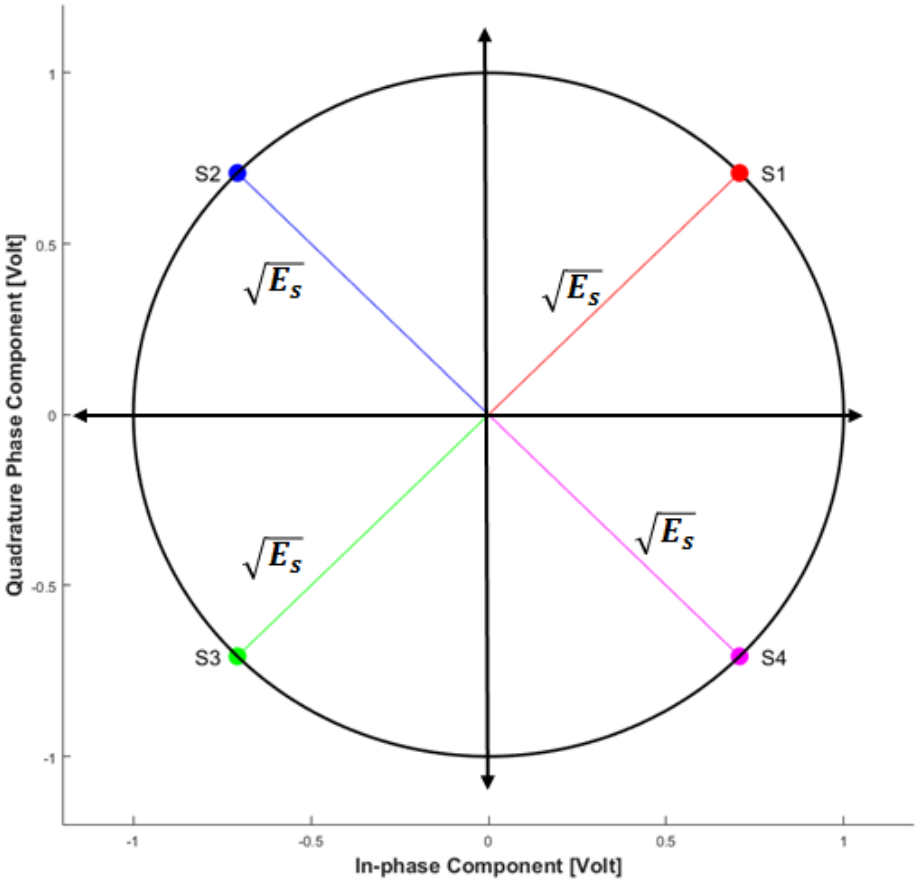

Figure 2.1: QPSK Signal Constellation

2.1.2 M-arry Amplitude Phase Shift Keying

In $MAPSK$ which is also known as $MQAM$, the information bits are mapped into symbols that are grouped based on different amplitudes and phases. In other words, a subset of the $MQAM$ symbols have the same amplitude but with different phases. The general $MQAM$ signal is as described by Eq. 2.9.

$$s_m(t) = [A_m * cos(\phi_m)p(t)cos\,(2\pi f_c t) - B_m * sin(\phi_m)p(t)sin\,(2\pi f_c t)] \tag{2.9}$$

where the two amplitudes A_m and B_m represent the $MQAM$ constellation′s components. One common $MQAM$ scheme is that has a square constellation as given by Eq. 2.10.

$$S_{i,j} = \sqrt{\frac{3E_s}{2\,(M-1)}}\left[\left(2i - 1 - \sqrt{M}\right) + j\left(2j - 1 - \sqrt{M}\right)\right] \tag{2.10}$$

$\forall i = 1, 2, ... \sqrt{M}, j = 1, 2, ..., \sqrt{M}$. The signal constellation of square $MQAM$ is shown in figure 2.2.

The modulation spectrum efficiency of square [16] $MQAM$ (l_{MQAM}) is given by:

$$l_{MQAM} = \sqrt{M} \tag{2.11}$$

In this thesis, $MPSK$ modulation scheme is used for the transmission of the information.

2.2 Gray Encoding

The mapping from bits to symbols is based on Gray encoding such that for each two adjacent symbols, there will be a change in one bit only [17]. This type of encoding will reduce the bit error rate (BER). Tables 2.1, 2.2, and 2.3 show the Gray encoding for $M = 4$,

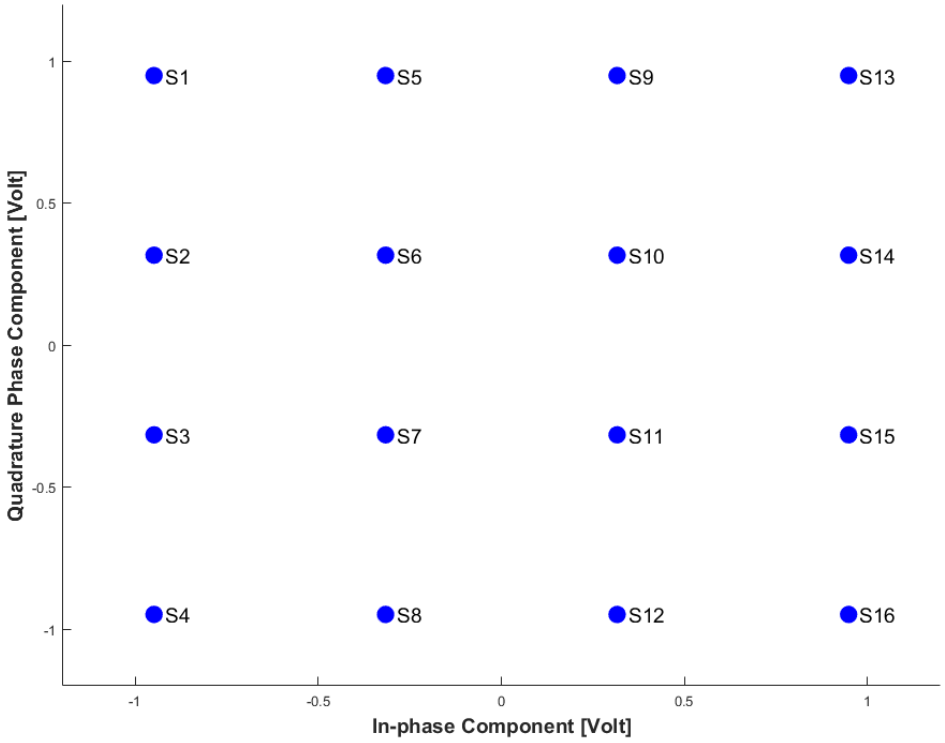

Figure 2.2: 16QAM Signal Constellation

$M = 8$, and $M = 16$ respectively.

Table 2.1: Gray Encoding for $M = 4$.

Information Bits	**Symbols**
0 0	$S1$
0 1	$S2$
1 1	$S3$
1 0	$S4$

Table 2.2: Gray Encoding for $M = 8$.

Information Bits	**Symbols**
0 0 0	$S1$
0 0 1	$S2$
0 1 1	$S3$
0 1 0	$S4$
1 1 0	$S5$
1 1 1	$S6$
1 0 1	$S7$
1 0 0	$S8$

Table 2.3: Gray Encoding for $M = 16$.

Information Bits	**Symbols**
0 0 0 0	$S1$
0 0 0 1	$S2$
0 0 1 1	$S3$
0 0 1 0	$S4$
0 1 1 0	$S5$
0 1 1 1	$S6$
0 1 0 1	$S7$
0 1 0 0	$S8$
1 1 0 0	$S9$
1 1 0 1	$S10$
1 1 1 1	$S11$
1 0 1 1	$S12$
1 0 1 0	$S13$
1 0 0 0	$S14$
1 1 0 0	$S15$
1 1 0 1	$S16$

2.3 Wireless Channel Model

Wireless transmission systems are classified into two categories as: Line of sight (LOS) and Non-Line of sight (NLOS) [18]. MIMO systems are NLOS wireless transmission schemes that are based on multi-path propagation [19]. In multi-path propagation, the transmitted signal arrives the receiver from different paths due to reflection, diffraction, and scattering. This means that multiple copies of the same signal arrive the receiver. These multiple signals can create either constructive interference or destructive interference [20] as illustrated in figure 2.3. One of the models for wireless MIMO channel is the complex Gaussian random process having zero mean and variance σ^2. This model is called the Rayleigh model which is used in this thesis. The probability density function of the magnitude of the Rayleigh channel is described by [21] as given in Eq. 2.12:

$$p\left(|h|\right) = \frac{h}{\sigma^2} \exp\left(\frac{-h^2}{2\sigma^2}\right) \tag{2.12}$$

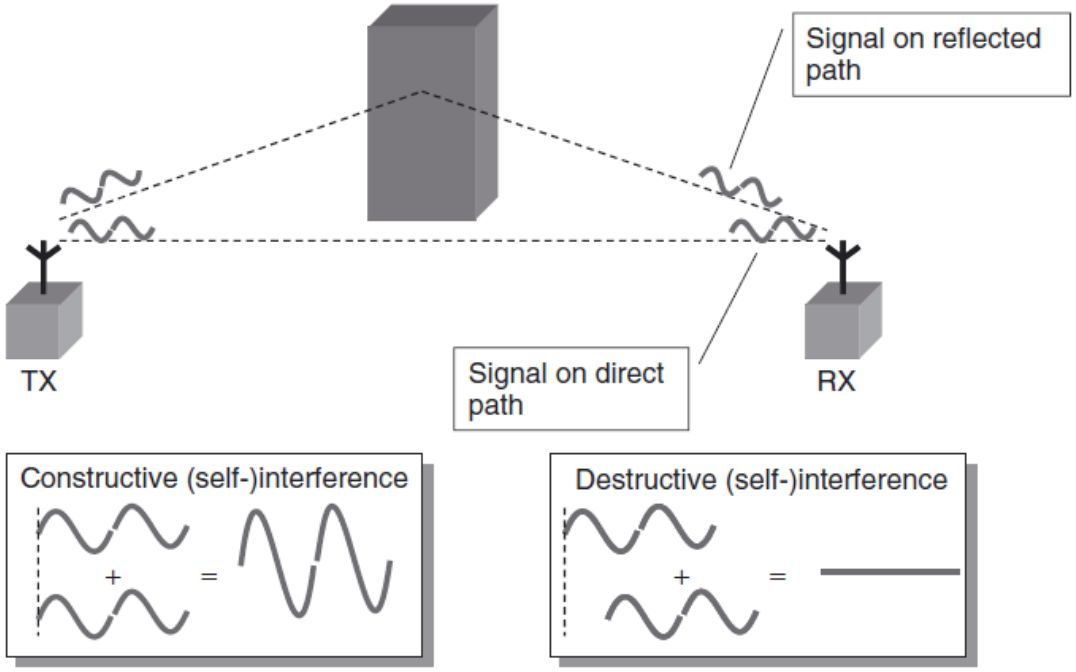

Figure 2.3: Multipath Propagation

The phase of the channel response is uniformly distributed between $-\pi$ and π.

2.4 MIMO Systems

MIMO system is based on the use of an N_t antennas at the transmitter, and an N_r antennas at the receiver. The notation $N_r \times N_t$ $MIMO$ is used to define the size of the MIMO system. For maximum spectrum efficiency, traditional $MIMO$ technologies are based on the multiple-symbol transmission where each transmit antenna has its own RF chain to transmit a different symbol. This requires that the number of receive antennas has to be equal or greater than the number of transmit antennas. Figure 2.4 shows the general block diagram of traditional $MIMO$ scheme. Channel matrix H is an $N_r \times N_t$ complex valued matrix that has to be estimated for the successful detection of the transmitted information.

Due to the simultaneous transmissions in $MIMO$ systems, each receive antenna receives

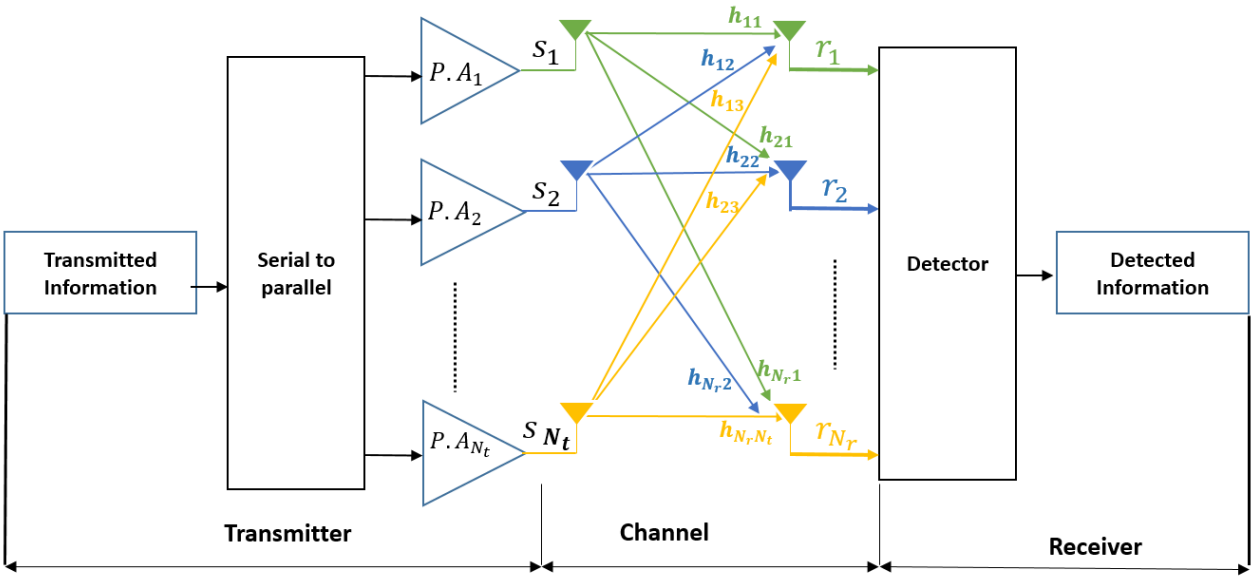

Figure 2.4: Block Diagram of $MIMO$ wireless network.

signals from all the transmit antennas. The receiver signals at the input of the detector are given by [22]:

$$\begin{bmatrix} r_1 \\ r_2 \\ \vdots \\ r_{N_r} \end{bmatrix} = \begin{bmatrix} h_{11} & h_{12} & h_{13} & \dots & h_{1N_t} \\ h_{21} & h_{22} & h_{23} & \dots & h_{2N_t} \\ \vdots & \vdots & \vdots & \ddots & \vdots \\ h_{N_r1} & h_{N_r2} & h_{N_r3} & \dots & h_{N_rN_t} \end{bmatrix} \begin{bmatrix} s_1 \\ s_2 \\ \vdots \\ s_{N_t} \end{bmatrix} + \begin{bmatrix} n_1 \\ n_2 \\ \vdots \\ n_{N_r} \end{bmatrix} \tag{2.13}$$

Equation 2.13 can be written in a simple form as given in Eq. 2.14:

$$\mathbf{r} = \mathbf{Hs} + \mathbf{n} \tag{2.14}$$

where **r** is the vector of the received signals, **s**, is the vector of the transmitted signals, and **n** is the vector of the noise, and **H** is the $MIMO$ channel matrix given by.

$$H = \begin{bmatrix} h_{11} & h_{12} & h_{13} & \dots & h_{1N_t} \\ h_{21} & h_{22} & h_{23} & \dots & h_{2N_t} \\ \vdots & \vdots & \vdots & \ddots & \vdots \\ h_{N_r1} & h_{N_r2} & h_{N_r3} & \dots & h_{N_rN_t} \end{bmatrix} \tag{2.15}$$

There are several issues in conventional $MIMO$ schemes [23,24,25] such as:

- Inter-Channel Interference (ICI) due to simultaneous transmissions.
- High receiver complexity to reduce the ICI.
- Each transmit antenna has its own RF equipment.
- Singularity of the channel matrix in the case of large number of receive antennas.
- The capacity of MIMO systems is limited by the $min\,(N_r, N_t)$.

The next chapter includes the spatial modulation schemes and shows that it is a useful scheme that resolves a lot of issues on the current MIMO wireless systems.

Chapter 3

Generalized Spatial Modulation

3.1 Introduction

Spatial modulation is a 3D constellation transmission scheme that has been proposed by [26] and achieves both the highest spectrum and energy efficiencies amongst all the existing wireless MIMO schemes. The main idea of spatial modulation is that the transmitted information are conveyed implicitly by the wireless channel (spatial constellation) and explicitly by the transmitted modulated signal (signal constellation). The spatial constellation is implemented by the selection of the active antennas that are used for the transmission of the constellation signals. This means that the incoming bit stream is split into two blocks named the "spatial bits" and the "constellation bits". Based on the sequence of the spatial bits one or more transmit antennas will be chosen for the transmission of the constellation signal. Spatial modulation is classified into three categories [13,27,28] based on the number of active antennas and the number of symbols to be transmitted as follows:

- Spatial Modulation (SM).
- Single Symbol Generalized Spatial Modulation (SS-GSM).
- Multiple Symbol Generalized Spatial Modulation (MS-GSM).

3.2 Spatial Modulation

In Spatial Modulation (SM), only one transmit antenna is used to transmit the constellation signal per each transmission. This requires that the number of the antennas at the transmitter has to be a power of 2 [13]. Since one antenna is selected out of an N_t antennas, the number of possible combinations that represent the size of the spatial constellation $(N_c)_{SM}$ is calculated as in Eq. 3.1.

$$(N_c)_{SM} = N_t \tag{3.1}$$

For an $N_r \times N_t$ $MIMO$ scheme, the spatial spectrum efficiency η_s for SM schemes is given by Eq. 3.2.

$$\eta_s = log_2 (N_c) \tag{3.2}$$

The modulation spectrum efficiency η_m is defined by:

$$\eta_m = log_2 (M) \tag{3.3}$$

where M is the modulation order (also called constellation size). The total spectrum efficiency is the sum of (3.2) and (3.3) and given by:

$$\eta_{SM} = log_2 (N_t) + log_2 (M) \tag{3.4}$$

Figure 3.1 shows the block diagram of SM scheme for an $2\times 5 MIMO$. There is no specific rule to select the active antenna, but table 3.1 shows the pattern of the spatial bits that are used to activate the antennas which is based on the incremental order of the binary to decimal bit mapping.

In a nutshell, SM achieves the maximum energy efficiency, but it does not achieve the

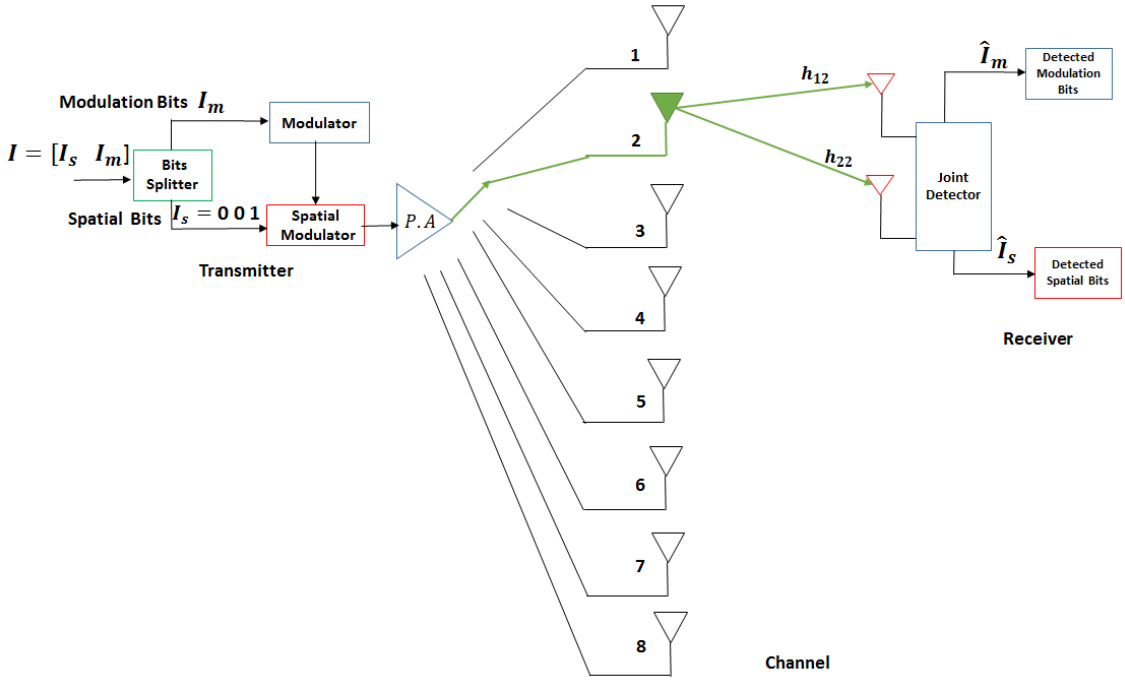

Figure 3.1: Block Diagram of SM for 2× 5 $MIMO$ scheme.

Table 3.1: Spatial Coding for $2 \times 8 MIMO$ SM scheme.

Spatial Bits	Active Antenna	Index of Spatial Channel Matrix
0 0 0	1	H_1
0 0 1	2	H_2
0 1 0	3	H_3
0 1 1	4	H_4
1 0 0	5	H_5
1 0 1	6	H_6
1 1 0	7	H_7
1 1 1	8	H_8

maximum spectrum efficiency in comparison to the other two types of spatial modulation schemes.

3.3 Generalized Spatial Modulation (GSM)

3.3.1 Spatial Model for GSM System

Generalized Spatial Modulation is based on that more one antenna are activated simultaneously for the transmission per each transmission period. The main advantage of GSM over SM is that the spatial constellation size is larger. This means that to achieve the same spatial spectrum efficiency, the number of transmitter antennas will be less than that for the SM. In addition, GSM resolves the constrain in SM about the number of antennas at the transmitter which is not necessary to be a power of 2. This means that GSM has more degree of freedom than SM in terms of the number of antennas at the transmitter. However, the constrain is that the spatial constellation size has to be a power of 2. Since there are N_a active antennas are selected out of an N_t antennas, the spatial constellation size N_c of GSM is given by [13]:

$$N_c = 2^{\lfloor log_2\left[\binom{N_t}{N_a}\right]\rfloor} \tag{3.5}$$

The spatial spectrum efficiency of $SS-GSM$ is (η_s) which is the same for $MS-GSM$, and it is given by:

$$\eta_s = \lfloor log_2\left[\binom{N_t}{N_a}\right]\rfloor \tag{3.6}$$

The maximum spatial spectrum efficiency is achieved when the number of multiple active antennas is the floor of the half of the number of the transmit antennas.

There is no specific rule for the spatial coding as in the case of SM. Table 3.2 explains the spatial coding for 2×5 $MIMO$ with 2 active antennas.

Table 3.2: Spatial Coding for 2×5 $MIMO$ GSM scheme.

Spatial Bits	Active Antennas	Index of Spatial Channel Matrix
0 0 0	1, 2	H_1
0 0 1	1, 3	H_2
0 1 0	1, 4	H_3
0 1 1	2, 3	H_4
1 0 0	2, 4	H_5
1 0 1	3, 4	H_6
1 1 0	3, 5	H_7
1 1 1	1, 5	H_8

3.3.2 Spatial Channel Matrix

The spatial channel matrix for GSM is a subset of the $MIMO$ channel matrix with the dimension of $N_r \times N_a$. The number of spatial channel matrices is equal to the size of the spatial constellation which is the number of all possible combinations of the active antennas. One of the tasks at the receiver is to detect which spatial channel matrix has been selected for the transmission of the modulation bits.

3.3.3 Single Symbol Generalized Spatial Modulation ($SS-GSM$)

Single Symbol Generalized Spatial Modulation ($SS-GSM$) is the most spectrum and energy efficient MIMO wireless technology. In $SS-GSM$ more than one transmit antenna are activated to transmit the same symbol at each transmission period. It keeps the same property as the SM where only one RF chain is needed with the advantage of higher spatial spectrum efficiency. The modulation spectrum efficiency of the $SS-GSM$ is the same as that of the SM. The total spectrum efficiency of $SS-GSM$ (η_{SS}) is as given in Eq. 3.7 [13].

$$\eta_{SS} = \lfloor log_2 \left[\binom{N_t}{N_a} \right] \rfloor + log_2 (M) \tag{3.7}$$

Figure 3.2 shows the block diagram of $SS-GSM$ for an 2×5 $MIMO$ according to the spatial coding given in Table 3.2. As shown in Figure 3.2, when the spatial bits sequence

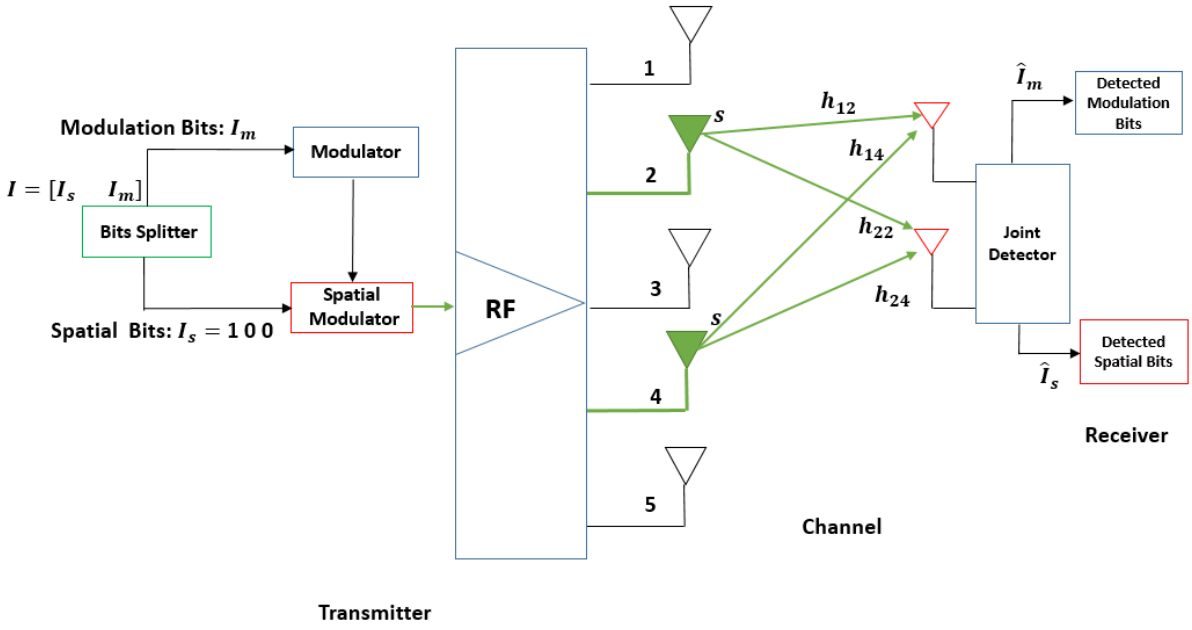

Figure 3.2: Block Diagram of SS-GSM for 2× 5 $MIMO$ scheme.

is "100", antenna2 and antenna4 are activated to transmit the signal of the modulation bits. The spatial channel matrix for this case is given by Eq. 3.8 as derived from (2.15).

$$H_5 = \begin{bmatrix} h_{12} & h_{14} \\ h_{22} & h_{24} \end{bmatrix} \tag{3.8}$$

One of the main characteristics of $SS-GSM$ is that it offers transmit diversity. Beside to the receive diversity of $MIMO$ schemes, a transmit diversity is implemented on $SS-GSM$ which helps to increase the robustness of the wireless channel quality.

3.3.4 Multiple Symbol Generalized Spatial Modulation

Multi-symbol generalzed spatial modulation MS-GSM is based on the transmission of N_a different symbols instead of transmitting the same symbol from the N_a active antennas to increase the modulation spectrum efficiency [28]. However, compared to the SS-GSM, MS-GSM is not energy efficient scheme where N_a of RF chains are required at the base station. In addition, there is no transmit diversity and there is an ICI at the receiver which degrades the performance. As we will see, because of the high computational complexity at the receiver, the throughput of the MS-GSM is less than than the SS-GSM even though it has higher spectrum efficiency. Figure 3.4 shows the block diagram for MS-GSM with 2 active antennas.

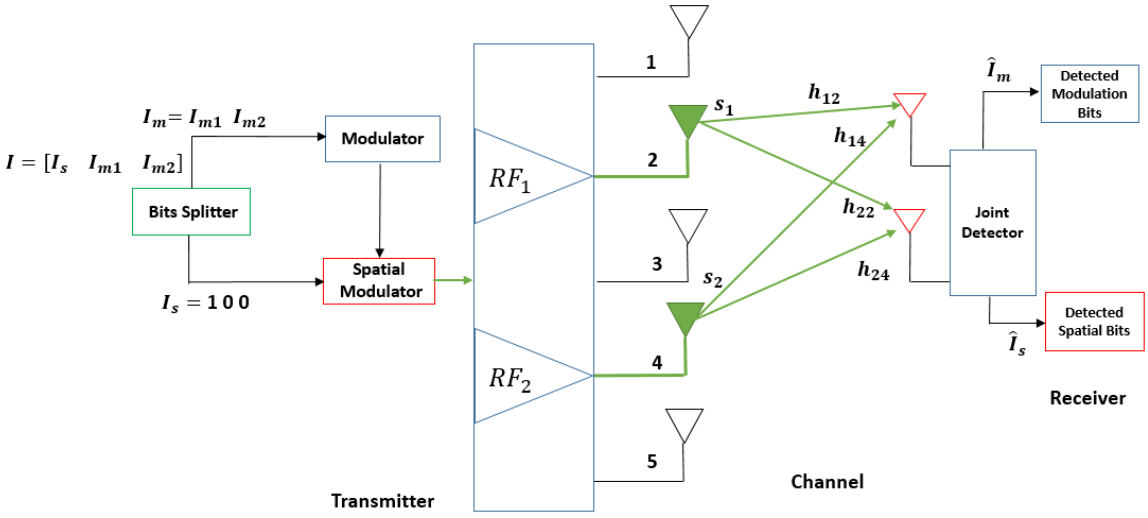

Figure 3.3: Block Diagram of MS-GSM for 2× 5 $MIMO$ scheme with $N_a = 2$.

The use of two RF chains RF_1 and RF_2 decreases the energy efficiency. In addition, there is no antenna diversity at the transmitter compared tho the case for $SS - GSM$.

The total spectrum efficiency of MS-GSM (η_{MS}) is calculated by Eq. 3.9.

$$(\eta)_{MS} = \lfloor log_2 \left[\binom{N_t}{N_a} \right] \rfloor + N_s * log_2 (M) \tag{3.9}$$

where $N_s = N_a$ is the number of different symbols to be transmitted from the N_a active antennas. For $SS - GSM$, $N_s = 1$.

Figure 3.4 shows a comparison of the total spectrum efficiency versus the number of active antennas for the different wireless MIMO networks for $Nt = 16$ and $M = 8$.

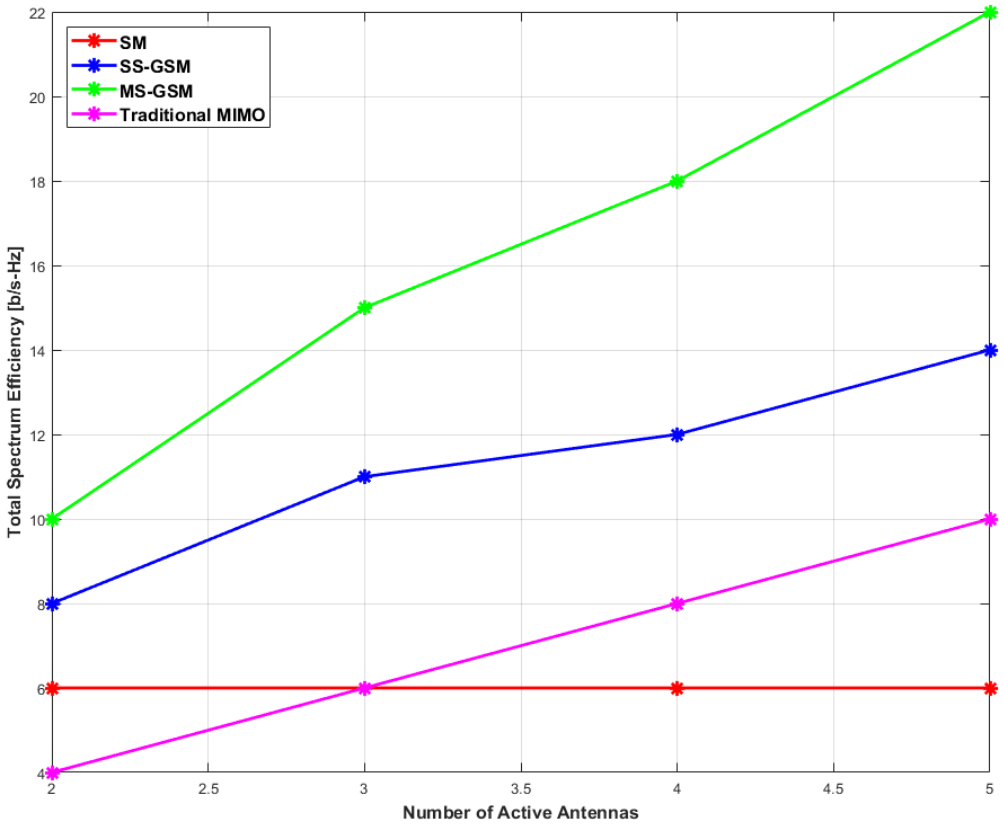

Figure 3.4: Total Spectrum Efficiency for $N_t = 16$ and $M = 8$.

Apparently, $MS - GSM$ offers the highest total spectrum efficiency as shown in (3.9)

compared to the spectrum efficiency on (3.7). However, and as will be explained latter, due to the high complexity for the detection process, the data transfer rate on $MS-GSM$ is lower compared to the $SS-GSM$.

3.4 Optimal Detection

Detection process in communication systems is a classification machine learning problem [29]. The task of the detector at the receiver is to classify the received signal′s symbol. After that symbol to bit mapping is applied to reconstruct the original data. The most common detection algorithm is the Maximum Likelihood (ML) detection algorithm that minimizes the loss function. The minimum loss function leads to the lowest bit error rate (BER). In SM,SS-GSM, or MS-GSM, the ML detection is a joint detection problem where both the index of the spatial channel matrix $\hat{j}$ and the index of the signal′s constellation $\hat{q}$ have to be estimated jointly. The ML detector is based on optimizing the mean square error.

3.4.1 ML Detection for SS-GSM schemes

The received signals′s vector $\mathbf{r}_{SS}$ is given by Eq. 3.10.

$$\mathbf{r}_{SS} = \left(\sum_{k=1}^{N_a} \mathbf{H}_j(:,k) \right) * s_q + \mathbf{n} \tag{3.10}$$

where $\mathbf{r}_{SS} \in \mathbb{C}^{N_r \times 1}$, $\mathbf{H_j} \in \mathbb{C}^{N_r \times N_a}$, $j = 1, 2, \ldots, \lfloor log_2 \left[\binom{N_t}{N_a} \right] \rfloor$ is the spatial channel matrix, $\mathbf{I}_{1 \times N_a}$ is a raw vector with all elements are equal to 1, s_q is the transmitted symbol with $q \in 1, 2, \ldots, M$, $\mathbf{n} \in \mathbb{C}^{N_r \times 1}$ is an AWGN vector. The elements of $\mathbf{H_j}$ and $\mathbf{n} \sim \mathbb{C}N(0, 1)$.

For simplicity, the $\sum_{k=1}^{N_a} \mathbf{H}_j(:,k)$ is defined as $\mathbf{h}_j$ as the spatial channel vector. The probability density function (pdf) of the received signal′s vector $P_r\left(\mathbf{r}_{SS}\backslash H_i, s_q\right)$ conditioned by H_j and s_q which is given by:

$$P_r\left(\mathbf{r}_{SS}\backslash H_i, s_q\right) = \frac{1}{(2\pi)^{\frac{N_r}{2}}\sqrt{|\sum|}} e^{-\frac{||\mathbf{r}_{SS} - \mathbf{h}_j \mathbf{s}_q||^2}{2\sum}} \tag{3.11}$$

The ML detector of (3.11) involves the joint estimation of the index of the spatial matrix of the active antennas (j)and the index of the transmitted symbol (q) that maximize (3.11), and it is given by Eq. 3.12 [13].

$$[j,q]_{SS} = \underset{\substack{j=1...,N_c \\ q=1...,M}}{\arg\min} ||\mathbf{r}_{SS} - \mathbf{h}_j s_q||^2 \tag{3.12}$$

3.4.2 ML Detection for MS-GSM schemes

The vector of the received signals $\mathbf{r}_{MS}$ for the $MS-GSM$ is expressed as:

$$\mathbf{r}_{MS} = \mathbf{H}_j \mathbf{x}_q + \mathbf{n} \tag{3.13}$$

where $\mathbf{x}_q \in \mathbb{C}^{N_s \times 1}$ with $q = 1, 2, ...M^{N_s}$. Each element on $\mathbf{x}_q \in$ the signal constellation of (2.3) or (2.10).

The optimum detection of (3.12) is similar to that for (3.10) and it is given by Eq. 3.13 [28].

$$[j,q]_{MS} = \underset{\substack{j=1...,N_c \\ q=1...,M^{N_a}}}{\arg\min} ||\mathbf{r}_{MS} - \mathbf{H}_j \mathbf{x}_q||^2 \tag{3.14}$$

3.5 Computational Complexity

The ML detectors of (3.12) and (3.14) involves the search over all the transmitter antennas, receiver antennas, and the signal constellations. This increases the computational complexity at the receiver, and therefore, increasing the power dissipation at the receiver and slow down the data transfer rate. The computational complexity includes the number of multiplications/divisions and summations/subtractions which is known in the field of deep learning as the number of floating point operations ($flops$). Researchers in the field of wireless communication are more concerning about the number of real valued multiplications than the number of summations.

The multiplication of two complex variables $(x_1 + jy_1)$ and $(x_2 + jy_2)$ involves four real valued multiplications which are calculated as follows: $[x_1 * x_2, x_1 * y_2, y_1 * x_2, y_1 * y_2]$ and 2 summations which are calculated as: $[x_1 * x_2 - y_1 * y_2, x_1 * y_2 + x_2 * y_1]$. Based on this concept, the computational complexity for the ML detection of $SS - GSM$ and $MS - GSM$ are calculated as follows:

3.5.1 Computational Complexity of SS-GSM

- The multiplication of $\mathbf{h}_j\mathbf{s}_q$ has $4N_r$ real valued multiplication and $2N_r$ summations per one spatial channel matrix per one signal constellation.
- The subtraction $\mathbf{r}_{SS} - \mathbf{h}_j\mathbf{s}_q$ has $2N_r$ subtractions per one spatial channel matrix per one signal constellation.
- The Euclidean norm $||\mathbf{r}_{SS} - \mathbf{h}_j\mathbf{s}_q||^2$ has $2N_r$ multiplications and N_r summations per one spatial channel matrix per one signal constellation.

Therefore, the total computational complexity of (3.12) has $6N_r$ multiplications and $5N_r$ summations per one spatial channel matrix per one signal constellation. Since the spatial size is N_c and the constellation size M, the total computational complexity for $SS-GSM$ in terms of $flops$ $(C_{SS})_{flops}$ and in terms of real valued multiplications $(C_{SS})_{RVM}$ are as given in Eqs. 3.15 and 3.16 respectively.

$$(C_{SS})_{flops} = 11N_r * \lfloor log_2 \left[\binom{N_t}{N_a} \right] \rfloor * M \tag{3.15}$$

$$(C_{SS})_{RVM} = 6N_r * \lfloor log_2 \left[\binom{N_t}{N_a} \right] \rfloor * M \tag{3.16}$$

3.5.2 Complexity of MS-GSM

- The multiplication of $\mathbf{H}_j\mathbf{x}_q$ in (3.14) has $4N_rN_a$ real valued multiplication and $2N_rN_a$ summations per one spatial channel matrix per one signal constellation.
- The subtraction $\mathbf{r}_{MS} - \mathbf{H}_j\mathbf{x}_q$ has $2N_r$ subtractions per one spatial channel matrix per one signal constellation.
- The Euclidean norm $||\mathbf{r}_{SS} - \mathbf{h}_j\mathbf{s}_q||^2$ has $2N_r$ multiplications and N_r summations per one spatial channel matrix per one signal constellation.

Therefore, the total computational complexity of (3.14) has $(4N_r * N_a + 2N_r)$ multiplications and $(2N_r * N_a + 3N_r)$ summations per one spatial channel matrix per one signal constellation. Since the spatial size is N_c and the constellation size M^{N_a}, the total computational complexity for $MS-GSM$ in terms of $flops$ $(C_{MS})_{flops}$ and in terms of real valued

multiplications $(C_{MS})_{RVM}$ are as given in Eqs. 3.15 and 3.16 respectively.

$$(C_{MS})_{flops} = (6N_r * N_a + 5N_r) * \lfloor log_2 \left[\binom{N_t}{N_a} \right] \rfloor * M^{N_a} \tag{3.17}$$

$$(C_{MS})_{RVM} = (4N_r * N_a + 2N_r) * \lfloor log_2 \left[\binom{N_t}{N_a} \right] \rfloor * M^{N_a} \tag{3.18}$$

Note that the computational complexity of $MS-GSM$ depends exponentially on the spatial constellation size.

Chapter 4

Deep Learning

4.1 Introduction

Deep learning is a machine learning based algorithm that can learn directly from data and perform a set of desired tasks. Machine learning is categorized mainly into three categories:

- Supervised Learning.
- Unsupervised Learning.
- Reinforcement Learning.

Supervised machine learning tasks are classification and regression. Examples of classification tasks include (but not limited) image classification, object detection and recognition, natural language processing, anomaly detection, and denoising [30, ch5]. Supervised learning is based on discriminant analysis which can be linear or nonlinear discriminant analysis [30]. This thesis is focused on the use of supervised machine learning for the estimation of the channel coefficients and the use of unsupervised learning for the detection process of the received symbols. These are implemented using Convolutional Neural Networks (CNN).

4.2 Artificial Neural Network

Artificial Neural Network is inspired from the human brain. The basic building block of an artificial neural network is called the perceptron that has multiple inputs and one output. as shown in Figure 4.1. Mathematically, the output of the neuron of figure 1 is expressed as:

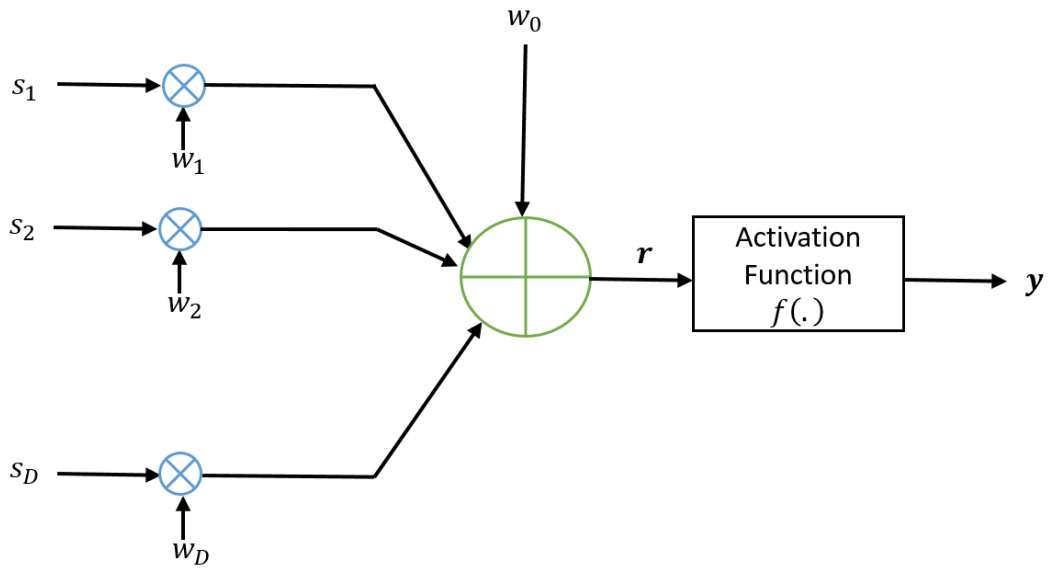

Figure 4.1: Single Perceptron Layer Artificial Neural Network.

$$y = f\left(\sum_{i=1}^{D} w_i s_i + w_0\right) \tag{4.1}$$

The activation function $f(.)$ is a linear or nonlinear mapping function that finds the activation of each neuron based on threshold level [32]: A Neural network is a multilayer

Table 4.1: Common Activation Functions.

Activation Function	**Mathematical Model**	**Range**
Linear	$f(x) = a * x$	$(-\infty, \infty)$
ReLU	$f(x) = max(0, x)$	$[0, \infty)$
tanh	$f(x) = tanh(x)$	$(-1, 1)$
Sigmoid	$f(x) = \frac{1}{1+e^{-x}}$	$(0, 1)$
Softmax	$f(x_i) = \frac{e^{x_i}}{\sum_{i=1}^{K} e^{x_i}}$	$(0, 1)$

perceptron (MLP) that has more than one layer and each layer consists of one or more neuron as shown in figure 4.2 where each circle represents the neuron of figure 4.1. Each neuron is called the unit of the layer. The first layer is called the input layer while the intermediate layers are called the hidden layer, and the output layer usually is used to determine the classes. This output layer can be fully connected or partially connected to the previous layer.

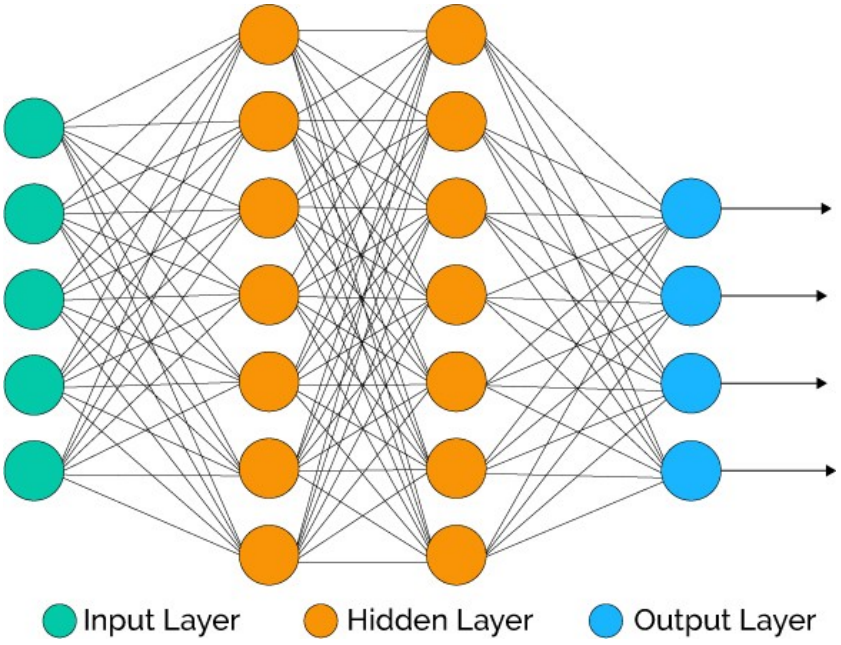

Figure 4.2: Multilayer Perceptron Artificial Neural Network [33]

As the signals propagate from one layer to another, useful information (also called features) are extracted. These features are used during the training of the NN′s model. Based on how the information are propagated from the input layer to the output layer, ANNs are classified as [34]:

- Feed Forward Neural Networks (FFNN).
- Recurrent Neural Network (RNN).

In FFNN, the information are propagated from the input layer to the output layer in one direction while in RNN, at least there is a feedback from one neuron to its input. In this thesis, one type of FFNN which is called Convolutional Neural Network (CNN).

4.3 Convolutional Neural Network

Convolutional neural network (CNN) is the most successful type of FFNN used for deep learning. It is based on the convolution operation in at least one layer for the extraction of features. CNN are used for any size of data tensors. The basic architecture of CNN consistes of the following layers and shown in figure 4.3:

- Convolution Layer
- Activation Layer
- Pooling Layer

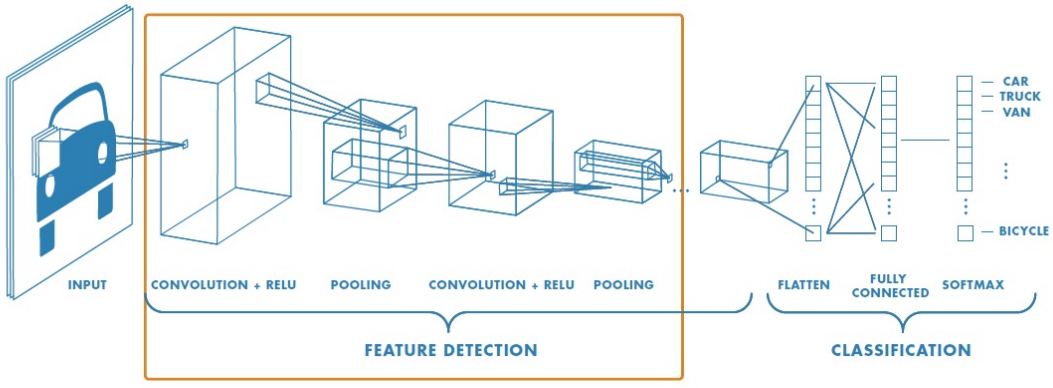

Figure 4.3: Multilayer Perceptron Artificial Neural Network [36]

On both the convolution and pooling layers, the dimensions of the extracted features are reduced. Maximum pooling function is widely used in CNNs.

4.4 Autoencoder Neural Network

An Autoencoder is a feed forward neural network that is used for data retrieval and dimensionality reduction [37]. The Autoencoder CNN consists of two main stages; the encoder stage and the decoding stage [38]. In this thesis, a denoising autoencoder (DAE) is used for the detection on wireless MIMO networks. The DAE is modeled by an encoder model that accepts input data $\mathbf{x}$ and introduce a corruption process having certain distribution to produce the corrupted information $\mathbf{C}(x)$ and perform the denoising process $g(c(x))$ to reproduce $\hat{x}$ which is a closer copy of x [30. ch14].

4.5 Related Work

As mentioned earlier, detection process in communication systems is a multi-class machine learning problem that uses maximum likelihood detection algorithm to reconstruct the transmitted information after processing and classifying the received signals. In GSM-MIMO systems, there are two sets of classes. One set of classes belongs to the signal constellation and the other set belongs to the spatial constellation.

Machine learning models are based on learning weights that minimize the cost function. Similarly, in wireless MIMO systems there are learning weight that can be learned to increase the system′s performance. These learning weights can be classified as:

- Transmit Power level: It can be learned through a feedback loop. The learning of transmit power level is usually known as automatic power control (AGC)
- Channel Coefficients: The can be learned by either open loop or feedback loop.

AGC requires a feedback from the receiver to the transmitter while CSI can be implemented through closed loop feedback which is known as transmit channel status information (TSCI) or it can be implemented without feedback so that it is known at the receiver only and hence it is called receiver channel status information (RCSI). Detection process can be also solved without CSI by two methods:

- Differential Non-Coherent Detection.
- Blind Detection.

In differential non-coherent detection, the channel is assumed to be constant for a block of transmission and there is no need to estimate the channel coefficients. For the two above methods, the loss function is high compared to the case of the CSI.

The application of neural networks and especially CNN in wireless MIMO- networks is a recent application. The authors in [39] addressed the machine learning algorithms and their possible applications for different tasks in next generation wireless networks such as energy learning, MIMO channel learning, and device to device networking, but they did not give a specific model about the detection process which is the fundamental task of any communication systems. In [15], the authors proposed a novel deep learning model for the physical layer of single input single output communication systems. They modeled the physical layer as an autho-encoder CNN model and introduce the complex valued NN because the communication signals can be treated as a complex valued signals. However, their model is not applied for MIMO systems. The authors in [40] used auto-encoder neural network on conventional MIMO with full and partial CSI at the transmitter. In addition to the low spectrum and energy efficiencies of conventional MIMO schemes used in [40],

the use of TCSI consumes more resources (bandwidth, power, and system complexity) at the transmitter and the receiver. In [41], the authors propose an auto-encoder deep learning detector for the detection of the transmitted signal in MIMO-OFDM. However, they did not consider the complexity of their proposed model. From equation 14 in [41], the lost function is much computational intensive than the complexity of the traditional ML detector with lower performance accuracy. In the literature review, there is no concern about reducing the complexity of the detection process or optimization on the resources consumption of wireless communication systems.

Chapter 5

PROPOSED AUTO-ENCODER BASED COMPLEX-VALUED CNN

5.1 Introduction

In this chapter, a novel and custom complex valued auto-encoder convolutional neural network (CV-AE-CNN) model for wireless MIMO networks is proposed. This proposed model can be used for the detection process for any wireless communication system such as single input single output (SISO), traditional multiple input multiple output (MIMO), SS-GSM MIMO, or MS-GSM MIMO. In addition, a modified CV-CNN model is proposed for the constant envelop signal constellation to reduce the computational complexity in terms of the number of real valued multiplications. Figure 5.1 shows the main architecture of the proposed AE-CNN for any wireless MIMO systems.

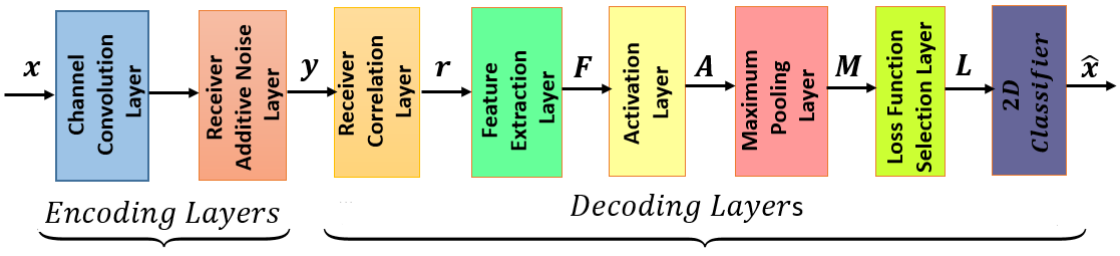

Figure 5.1: Block Diagram of the proposed AE-CNN

5.2 System Model

The following subsections include descriptions of the layers of the proposed CNN model.

5.2.1 Encoder Model

MIMO wireless channel is a multipath channel. One common model for MIMO channels is the Rayleigh fading model where the channel coefficients are assumed to be independent and identical, distributed (iid) Gaussian random process having zeros mean and unity variance. The channel and the AWGN at the receiver represent the encoder part that changes randomly both the amplitude and the phase of the transmitted signals. Unlike the traditional encoders which are bit level encoders and predesigned, channel and noise layers are uncontrolled. This means that their effect can't be avoided.

5.2.2 Receiver Correlation Layer

Receiver correlation layer is basically used to extract the in-phase and quadrature components of the received signals **y**. In practical systems, the complexed valued received signal at the output of this layer **r** can be obtained using correlation receiver, and it is given by Eq. 5.1.

$$\mathbf{r} = \int_0^T \mathbf{y}(t).\psi_{\mathbf{1}}(t) + j \int_0^T \mathbf{y}(t).\psi_{\mathbf{2}}(t) \tag{5.1}$$

where $\mathbf{y}(t)$ is the time domain of the received signals and $\psi(t)$ is the time domain of the orthonormal signals that are given in Eqs 2.6 and 2.7. The time domain low pass equivalent model of the received signals is given by Eq 5.2.

$$\mathbf{y}(t) = \mathbf{s}(t) * \mathbf{h}(t) + \mathbf{n}(\mathbf{t}) \tag{5.2}$$

In simulation and to save the PC resources, equations 2.14, 3.10 or 3.13 are used instead of Eq 5.2.

5.2.3 Supervised learning for Channel coefficients

The channel coefficient h_{ik} in the channel matrix given in (2.15) can be estimated by transmitting a pilot symbol s_p from the k^{th} transmit antenna and received by the i^{th} antenna for $i = 1, 2, ...N_r$. This pilot symbol is known to the receiver, and this process is commonly known in the field of communications as channel estimation using pilot symbols while in the field of machine learning is known as training the model. The channel coefficients are learned as given in Eq. 5.3.

$$h_{i,k} = \frac{r_i, k}{conj(s_p)} \tag{5.3}$$

where $k = 1, 2, N_t$

5.2.4 Features Extraction Layers

In this layer, features are extracted from the pre-defined signal constellation and channel coefficients. The output of this layer has the dimensionality of $N_r \times N_c \times M$. For SS-GSM schemes, two different Features extraction algorithms are used in this thesis. The first algorithm is the traditional algorithm that commonly used in the literature and the second algorithm is proposed to reduce the computational complexity in terms of the number of real valued multiplications.

Traditional Features Extraction algorithm

The features extraction algorithm for SS-GSM $(\mathbf{F}_{SS})_T$ is given by Eq. 5.4

$$(\mathbf{F}_{SS})_T = \mathbf{r}_{SS} - \mathbf{h}_j s_q \tag{5.4}$$

$\forall i = 1, 2, ..., N_r$ and $\forall j = 1, 2, ...N_c$, $q = 1, 2, ..., M$, and $\mathbf{h_j}$ is the spatial channel vector which is given by Eq 5.5.

$$\mathbf{h}_j = \sum_{k=1}^{N_a} \mathbf{H}_j(:, k) \tag{5.5}$$

The features extraction algorithm for MS-GSM $(\mathbf{F}_{MS})_T$ is given by Eq. 5.6

$$\mathbf{F}_{MS} = \mathbf{r}_{MS} - \mathbf{H}_j \mathbf{x_q} \tag{5.6}$$

$\forall i = 1, 2, ..., N_r$ and $\forall j = 1, 2, ...N_c$, $q = 1, 2, ..., M^{N_a}$. The extracted features in Eq. 5.4 and 5.6 represent the different between the observed signals and the transmitted signals multiplied by the channel coefficients. In other words, they represent the complex valued error due to the noise components at the receiver.

Proposed Features Extraction Method

The proposed features extraction algorithm for SS-GSM $(\mathbf{F}_{SS})_P$ is given by Eq. 5.7.

$$(\mathbf{F}_{SS})_P = \frac{s_q^* \mathbf{r}_{SS}}{|s_q|} - \mathbf{h}_j \tag{5.7}$$

From Eq.3.12, the maximum likelihood detection of the proposed features extraction in Eq.5.6 is give by Eq. 5.8.

$$[j, q]_{SS(ML)} = \underset{\substack{j=1...,N_c \\ q=1...,M}}{\arg\min} || \frac{s_q^* \mathbf{r}_{SS}}{|s_q|} - \mathbf{h}_j ||^2 \tag{5.8}$$

Note that the extracted features represent the complex valued error.

5.2.5 Activation Layer

The absolute value is chosen to be the activation function for this layer. This activation function is applied to the in-phase component and quadrature phase component separately.

The outputs of this layer are given by Eq 5.9 and 5.10.

$$\mathbf{A_R} = |\Re(\mathbf{F})| \tag{5.9}$$

$$\mathbf{A_I} = |\Im(\mathbf{F})| \tag{5.10}$$

where $\mathbf{F}$ can be as given by Eqs. 5.4, 5.6, or 5.7. The reason for choosing the absolute value as an activation function that separately applied on the real and imaginary components is that because the extracted features represent the error values in which one spatial channel and one selected symbol give jointly the minimum error. The output of this layer is still a 3D space.

5.2.6 Maximum Pooling

As mentioned in chapter 4, maximum pooling is used for dimensionality reduction. In the proposed model, the maximum pooling layer will select the maximum value of the activation function of the real part and the imaginary part independently amongst all the receive antennas. This means that the output of the maximum pooling layer is the maximum absolute error on the in-phase and quadrature phase components. The output space of this layer M has a dimensionality of $N_c \times M$, and are given as shown in Eq. 5.11 and 5.12.

$$\mathbf{M_R} = \max(|\Re(\mathbf{F})|) \tag{5.11}$$

$$\mathbf{M_I} = \max(|\Im(\mathbf{F})|) \tag{5.12}$$

5.2.7 Loss Function

The proposed loss function is selected to be the first norm of the output of the maximum pooling layer which is basically the sum of the maximum of the absolute value of the real

part of the error and the maximum of the absolute value of the imaginary part of the error, and it is given by:

$$\mathbf{L}(j,q) = \max\left(|\Re\left(\mathbf{F}\right)|\right) + \max\left(|\Im\left(\mathbf{F}\right)|\right) \tag{5.13}$$

In the case of traditional extracted features for $SS-GSM$, the loss function will be

$$(\mathbf{L_{SS}})_T = \max\left(|\Re\left(\mathbf{r}_{SS} - \mathbf{h}_j s_q\right)|\right) + \max\left(|\Im\left(\mathbf{r}_{SS} - \mathbf{h}_j s_q\right)|\right) \tag{5.14}$$

For the proposed extracted features in Eq. 5.7, the loss function is given as:

$$(\mathbf{L_{SS}})_P = \max\left(|\Re\left(\frac{s_q^*\mathbf{r}_{SS}}{|s_q|} - h_j\right)|\right) + \max\left(|\Im\left(\frac{s_q^*\mathbf{r}_{SS}}{|s_q|} - h_j\right)|\right) \tag{5.15}$$

For $MS-GSM$, the loss function will be:

$$\mathbf{L_{MS}} = \max\left(|\Re\left(\mathbf{r}_{SS} - \mathbf{H}_j\mathbf{x_q}\right)|\right) + \max\left(|\Im\left(\mathbf{r}_{SS} - \mathbf{H}_j\mathbf{x}_q\right)|\right) \tag{5.16}$$

5.2.8 Classification Layer

The classification layer will estimate jointly the spatial channel matrix $\hat{j}$ and the index of the symbol $\hat{q}$ that minimize the loss function of Eq. 5.14, 5.15, or 5.16. Therefore, the solutions of the above three optimization problems are given by equations 5.17,5.18, and 5.19 respectively.

$$[\hat{j},\hat{q}]_{SS} = \underset{\substack{j=1\ldots,N_c\\ q=1\ldots,M}}{\arg\min}\left[\max\left(|\Re\left(\mathbf{r}_{SS} - \mathbf{h}_j s_q\right)|\right) + \max\left(|\Im\left(\mathbf{r}_{SS} - \mathbf{h}_j s_q\right)|\right)\right] \tag{5.17}$$

$$[\hat{j},\hat{q}]_{SS} = \underset{\substack{j=1\ldots,N_c\\ q=1\ldots,M}}{\arg\min}\left[\max\left(|\Re\left(\frac{s_q^*\mathbf{r}_{SS}}{|s_q|} - h_j\right)|\right) + \max\left(|\Im\left(\frac{s_q^*\mathbf{r}_{SS}}{|s_q|} - h_j\right)|\right)\right] \tag{5.18}$$

$$[\hat{j},\hat{q}]_{MS} = \underset{\substack{j=1...,N_c \\ q=1...,M}}{\arg\min} \left[\max\left(|\Re\left(\mathbf{r}_{MS} - \mathbf{H}_j\mathbf{x_q}\right)|\right) + \max\left(|\Im\left(\mathbf{r}_{MS} - \mathbf{H}_j\mathbf{x}_q\right)|\right)\right] \tag{5.19}$$

In other words, the de-noising CV-CNN is based on the minimum of the maximum error.

5.3 Computational Complexity

The computational complexity of the proposed CNN is calculated in a similar way for the calculation of the computational complexity presented in section 3.5.

5.3.1 Traditional SS-GSM

The extracted features on Eq. 5.4 include the following mathematical operations:

1. The product $\mathbf{h}_j s_q$ has $4N_r$ multiplications and $2N_r$ summations per spacial channel matrix per symbol with a search space of $N_r \times N_c \times N$.

2. $\mathbf{r_{SS}} - \mathbf{h}_j s_q$ has $2N_r$ summations per spatial channel matrix per symbol with a search space of $N_r \times N_c \times N$.

3. The maximum pooling layer will output a search space of $N_c \times M$.

4. The calculated loss function in Eq. 5.14 has one summation operation per spatial channel matrix per symbol with a search space of $N_c \times M$.

Therefore, the total computational complexity of Eq 5.16 in terms of the number of floating point operations $[(C_{SS})_T]_{flops}$ is sum of the complexities in the above steps and it is given by Eq. 5.20 while the computational complexity of Eq.5.17 in terms of real valued multiplications $[(C_{SS})_T]_{RVM}$ is given by 5.21.

$$[(C_{SS})_T]_{flops} = (8N_r + 1) * \lfloor log_2\left[\binom{N_t}{N_a}\right]\rfloor * M \tag{5.20}$$

$$[(C_{SS})_T]_{RVM} = 4N_r * \lfloor log_2 \left[\binom{N_t}{N_a} \right] \rfloor * M \tag{5.21}$$

5.3.2 Proposed SS-GSM

In a similar way to the previous subsection, the computational complexity of Eq.5.18 is calculated as follows:

1. The product $\frac{s_q^*}{|s_q|^2}$ is predetermined and does not cost any complexity during the detection process.
2. The product $\frac{s_q^* \mathbf{r}_{SS}}{|s_q|^2}$ has $4N_rM$ multiplications and $2N_rM$ summations.
3. The subtraction $\frac{s_q^* \mathbf{r}_{SS}}{|s_q|^2} - \mathbf{h}_j$ has only $2N_rN_cM$ summation operations.
4. The maximum pooling layer will output a search space of $N_c \times M$.
5. The calculated loss function in Eq. 5.14 has one summation operation per spatial channel matrix per symbol with a search space of $N_c \times M$.

From the above explanation, the total computational complexity of the proposed feature extraction layer $[(C_{SS})_P]_{flops}$ is the sum of the complexities in steps 2,3,and 5, it is given in Eq.5.22.

$$[(C_{SS})_P]_{flops} = 6N_rM + (2N_r + 1) \lfloor log_2 \left[\binom{N_t}{N_a} \right] \rfloor M \tag{5.22}$$

The computational complexity on Eq. 5.18 in terms of the real valued multiplications $[(C_{SS})_P]_{RV}$ is given by Eq. 5.23.

$$[(C_{SS})_P]_{RV} = 4N_r * M \tag{5.23}$$

It is clear that in the extracted feature on Eq.5.18, the multiplication operations do not

depend on the spatial dimension. This means that the total spectrum efficiency can be increased without increasing the complexity.

To calculate the total complexity of the proposed ML detector of Eq.5.8, the complexity of the norm operation which has $2N_rN_cM$ multiplications and N_rN_cM summations has to be added to the complexities on steps 2 and 3. Therefore, the total computational complexity of the proposed ML detector is as given in Eq 5.24

$$[(C_{SS-ML})_P] = \left(6 + 5\lfloor log_2 \left[\binom{N_t}{N_a}\right]\rfloor\right) N_rM \tag{5.24}$$

5.3.3 Complexity of MS-GSM

The computational complexity for the proposed model for MS-GSM is calculating as follows:

1. The product $\mathbf{H}_j\mathbf{x}_q$ is a multiplication of matrix of size $N_r \times N_a$ with a vector of $N_a \times 1$. Therefore , the total complexity for this product has $4N_rN_a$ multiplications and $2N_rN_a$ summations per one spatial matrix per one symbol′s vector.

2. The subtraction $\mathbf{r}_{MS} - \mathbf{H}_j\mathbf{x}_q$ has $2N_r$ summations.

3. The loss function in Eq. 5.19 has one summation per one spatial matrix per one symbol′s vector.

The total computational complexity is the sum of the complexities in the above three steps multiplied by the spatial and constellation search spaces ($N_c * M^{N_a}$) and it is given in Eq. 5.25.

$$C_{MS} = \left(6N_rN_a + 2N_r + 1\lfloor log_2 \left[\binom{N_t}{N_a}\right]\rfloor\right) N_rM^{N_a} \tag{5.25}$$

Chapter 6

Results

6.1 Computational Complexity

A comparison between the computational complexity at the receiver measured in terms of the total number of floating point operations versus the spatial efficiency (spatial constellation size) at modulation order of 8 between Eq 3.16 (Traditional ML detector), Eq. 5.20 (Proposed AE-CV-CNN of the traditional ML detector), Eq 5.24 (Proposed ML detector), and Eq 5.22 (Proposed AE-CV-CNN of the proposed ML detector) is shown in figure 6.1 a. The same computational complexity comparison but versus the signal constellation size (Modulation order) at a spatial constellation size of 8 is shown in figure 6.1 b. In the two comparisons, the number of active antennas is 2.

From figures 6.1 a and 6.1 b, the computational complexity for the proposed AE-CNN is lower than the complexity of the traditional ML detector. The two proposed models for feature extraction give lower complexity. In addition, the proposed ML detector achieve complexity less than the proposed $AE-CV-CNN$ of the traditional ML detector. The reduction on the total computational complexity is decreased as the total spectrum efficiency increased.

Numerical comparisons for the reduction of the computational complexity with respect

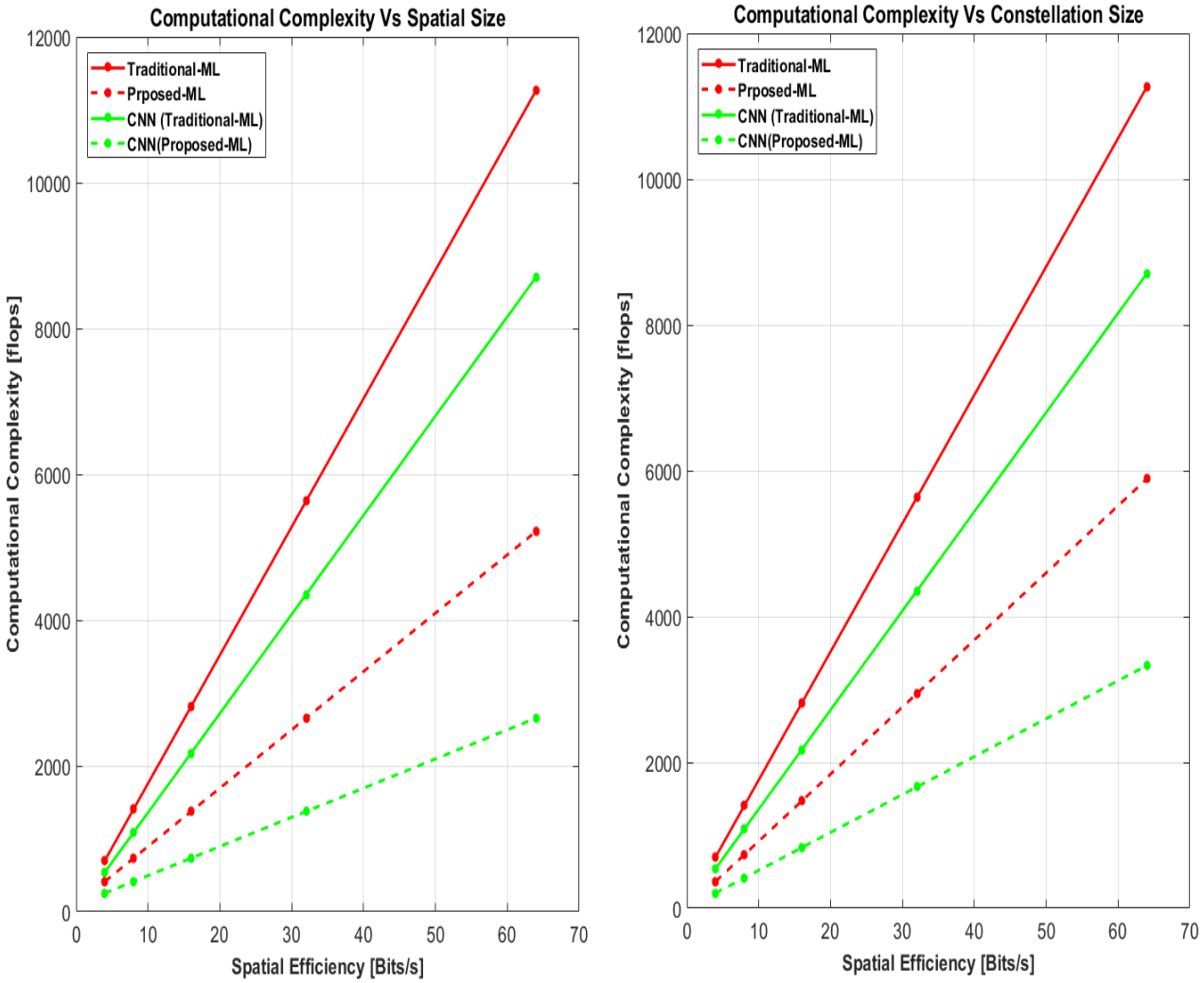

Figure 6.1: SS-GSM Computational Complexity Comparison versus Spatial size for $Nr = 2$. (a) $M = 8$ and N_c is variable. (b) $N_c = 8$ and M is variable.

to the complexity of the traditional ML detector for the above comparisons are given in tables 6.1 and 6.2.

Table 6.1: SS-GSM Spatial Complexity Reduction Ratio for $M = 8$.

N_c	**CNN(Traditional ML)**	**Proposed ML**	**CNN(Proposed ML)**
4	22.73%	40.91%	63.64%
8	22.73%	47.73%	70.45%
16	22.73%	51.14%	73.86%
32	22.73%	52.84%	75.57%
64	22.73%	53.69%	76.42%

Table 6.2: SS-GSM Modulation Complexity Reduction Ratio for $N_c = 8$.

M	CNN(Traditional ML)	Proposed ML	CNN(Proposed ML)
4	22.73%	47.73%	70.45%
8	22.73%	47.73%	70.45%
16	22.73%	47.73%	70.45%
32	22.73%	47.73%	70.45%
64	22.73%	47.73%	70.45%

From tables 6.1 and 6.2, the achieved complexity reduction is quite significant for the proposed ML detector and the CNN applied for it. An other feature is that the spatial domain offers higher reduction than the constellation domain.

Figure 6.2 shows a comparison of the computational complexity in terms of real valued multiplications for the same system configuration of figure 6.1.

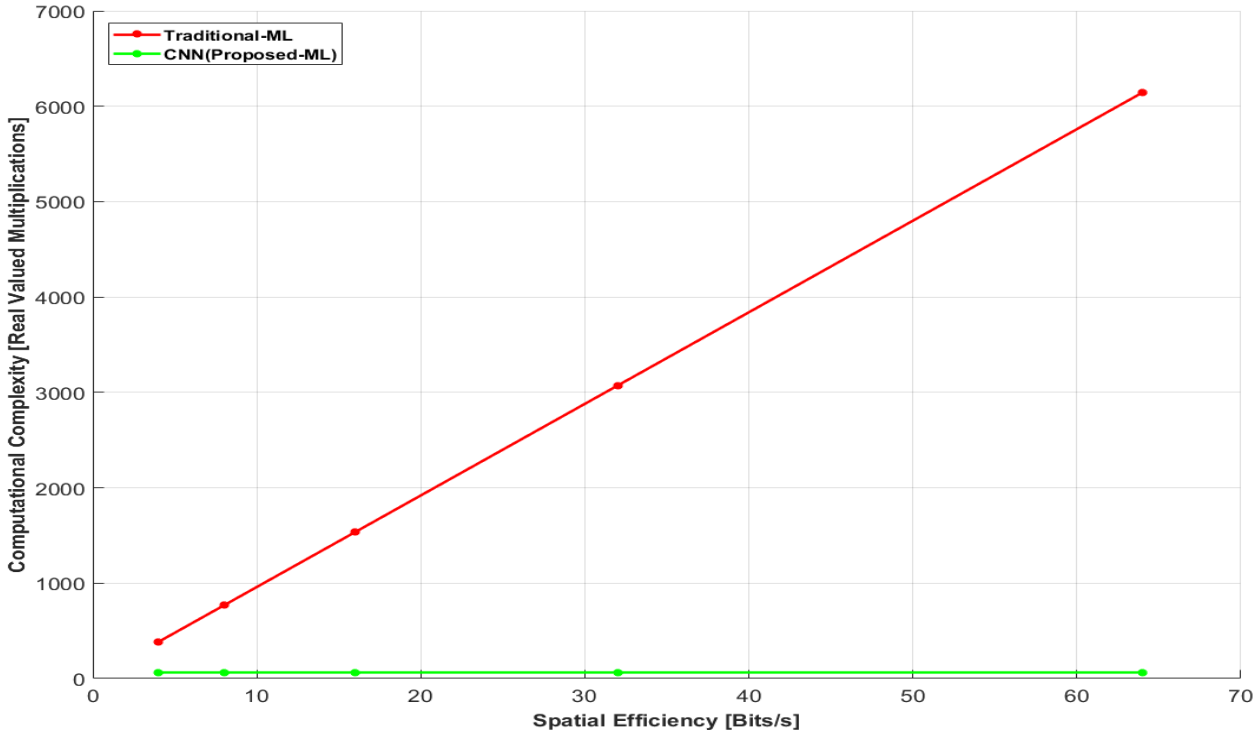

Figure 6.2: SS-GSM Comparison of Computational Complexity in terms of real valued multiplications: Nr=2, M=8

Since the computational complexity in terms of the number of real valued multiplications is independent on the spatial modulation, the complexity reduction is very high. In other words, the relative complexity relative to the ML detector is very low as it can be seen from figure 6.2.

For the MS-GSM systems, the computational complexity for the ML detector given by Eq. 3.18 and the proposed model given by Eq. 5.25 are shown in figure 6.3.

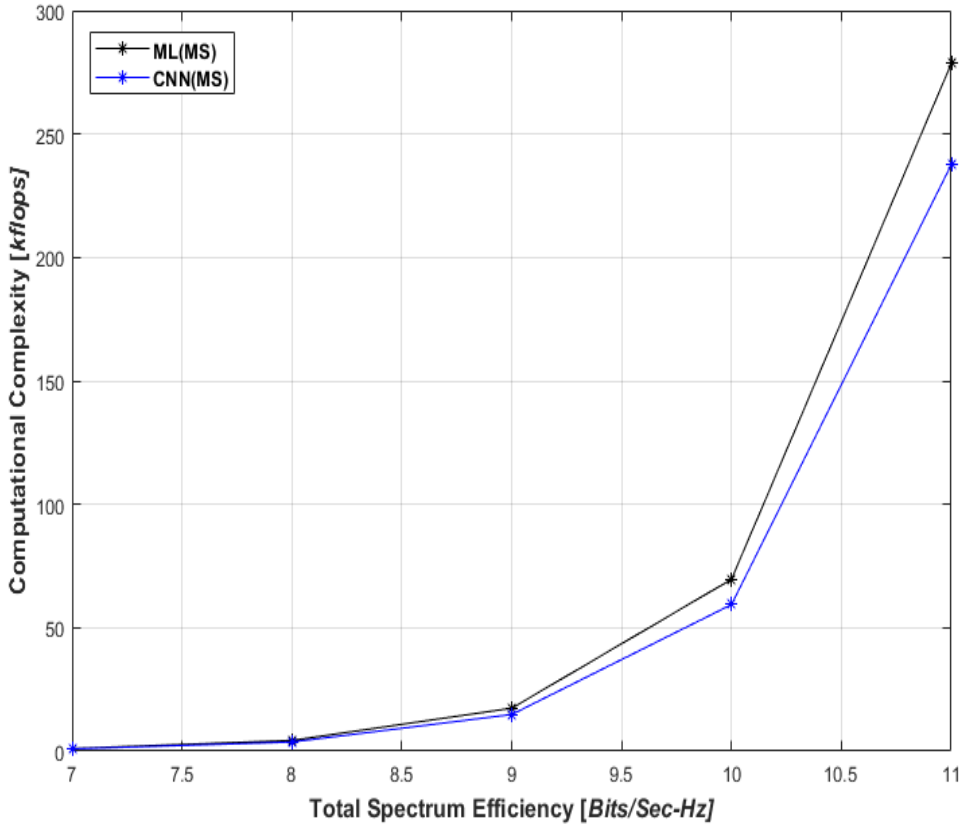

Figure 6.3: MS-GSM Comparison of Computational Complexity in terms of real valued multiplications: Nr=2, M=8

6.2 Performance

In this section, the performance of the receiver in terms of the accuracy, bit error rate, scatter plots of the separable classes, and the confusion matrix are examined.

6.2.1 SS-GSM system

Accuracy

The performance accuracy of the detection process for the SS-GSM is as shown in figure 6.4 where the modulation scheme is 8PSk and the $N_a = 2$. The accuracy comparison includes the computationally intensive traditional ML detector, the proposed CV-CNN for the traditional ML detection, the proposed low cost ML detector, and the proposed CV-CNN for the proposed ML detector.

From figure 6.4, the value of SNR=20 dB which represents the learned transmission power level can be considered as the optimum transmission power level where the accuracy is about 99.4%.

Bit Error Rate

The bit error rate which is the metric of the detector′ performance is shown in figure 6.5. The bit error rate is relatively high for $SNR < 23dB$. This is because of the learned channel coefficients using lower transmission power. The data used for the learning of the channel coefficients (analogy to training model) is extremely lower than the user data. Therefore, higher transmission power ($SNR > 26dB$) can be used for the channel estimation to reduce the bit error rate. This provides the flexibility to reduce the transmission power during the transmission of the user data.

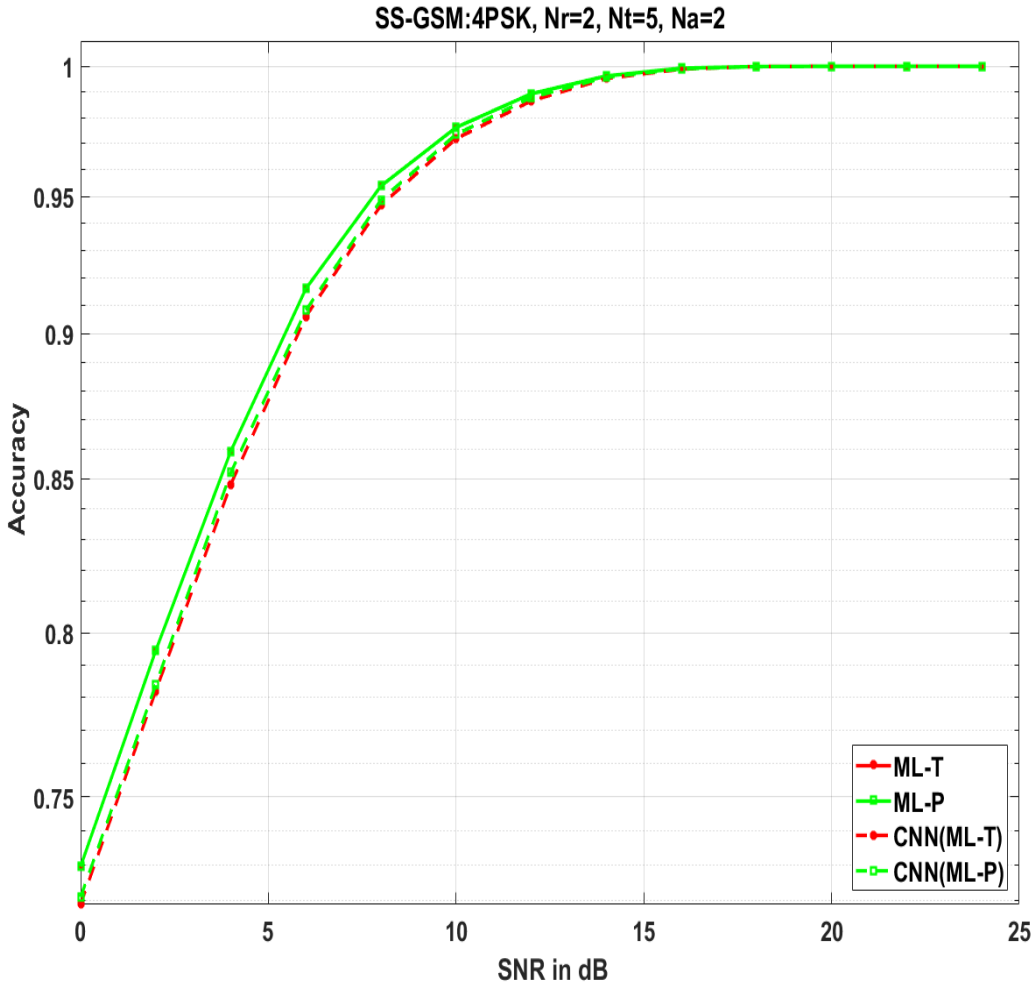

Figure 6.4: SS-GSM Confusion Matrix for the QPSK transmitted Symbols.

Scatter Plotting

In figure 6.6, the scatter plot of the received signals′ vector with out the learning spatial channels at SNR of 18*db*. Without learning the channel status, the symbols′ classes are overlapped, and it is impossible to detect the actual transmitted symbol.

Figures 6.7, 6.8 show the scatter plot of the projection of the received vector on the

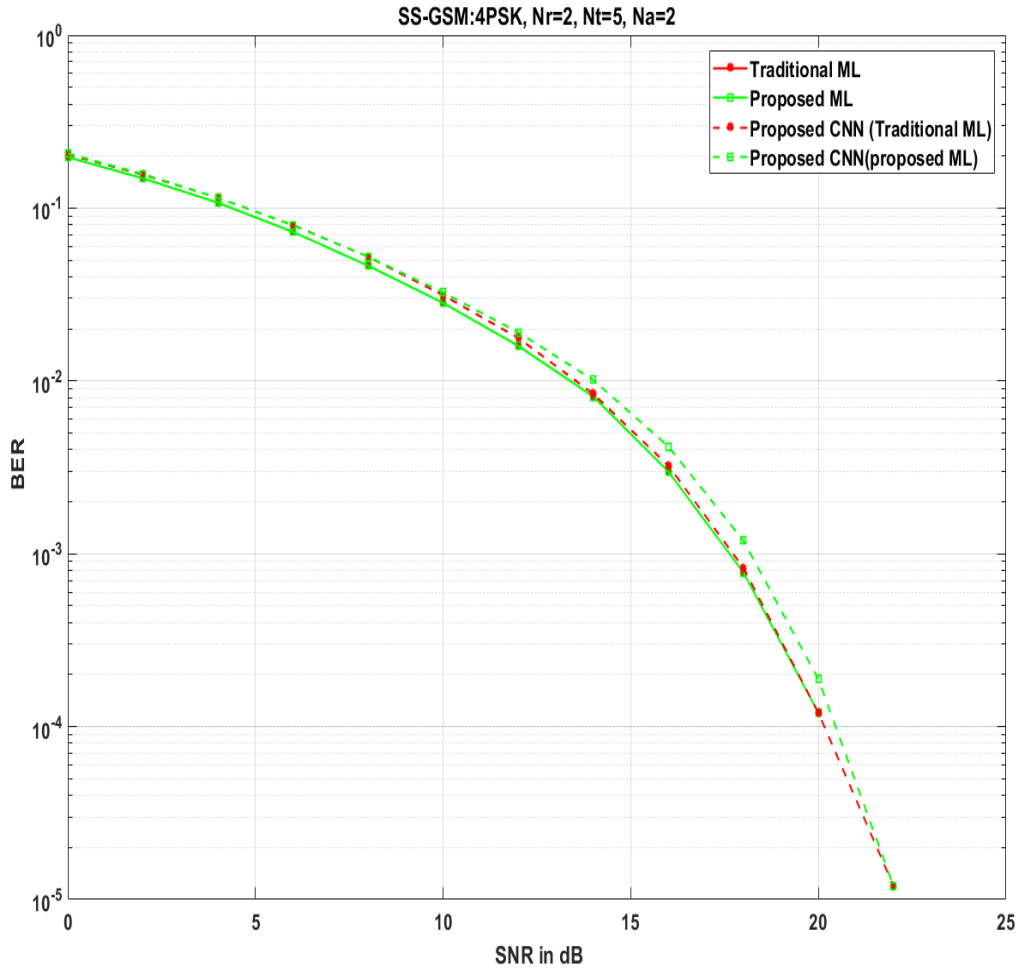

Figure 6.5: SS-GSM Bit Error Rate.

learned spatial channel vectors given in Eq 5.5 using the proposed CC-CNN of the traditional ML detector for the learned transmission power levels corresponding to the SNR values of 6,8,16,and 18 dB respectively.

Figures 6.9 and 6.10 shows the same as in figures 6.7 and 6.8 using the proposed CV-CNN for the proposed ML detector.

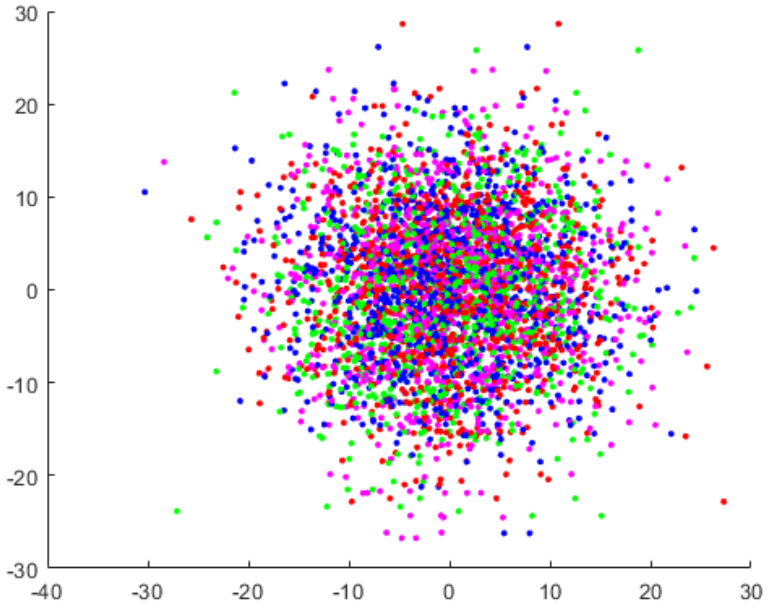

Figure 6.6: Scatter plot of the received signals at SNR of 18dB.

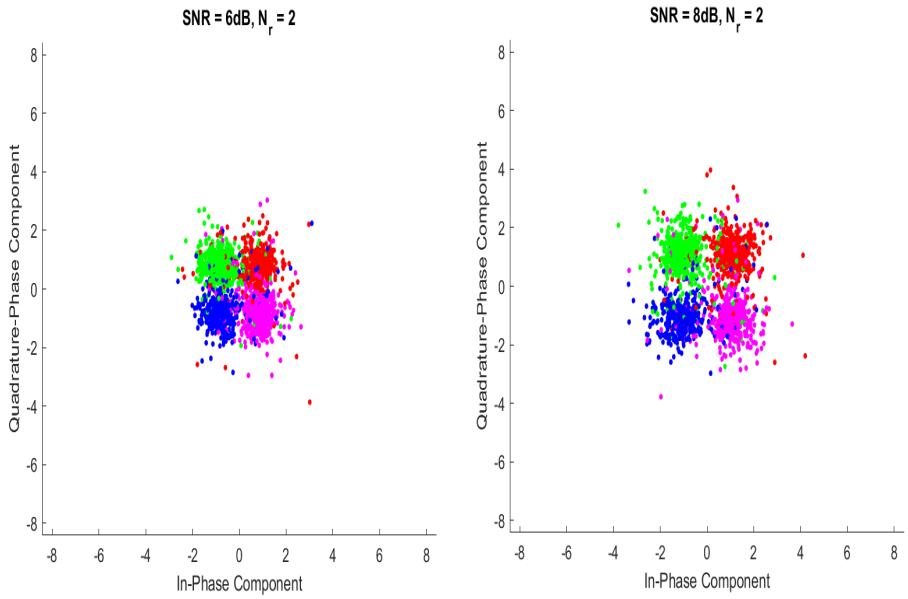

Figure 6.7: SS-GSM Scatter plot of the projection of the received vector on the learned channel using CNN(Traditional ML) at SNR of 6dB and 8dB

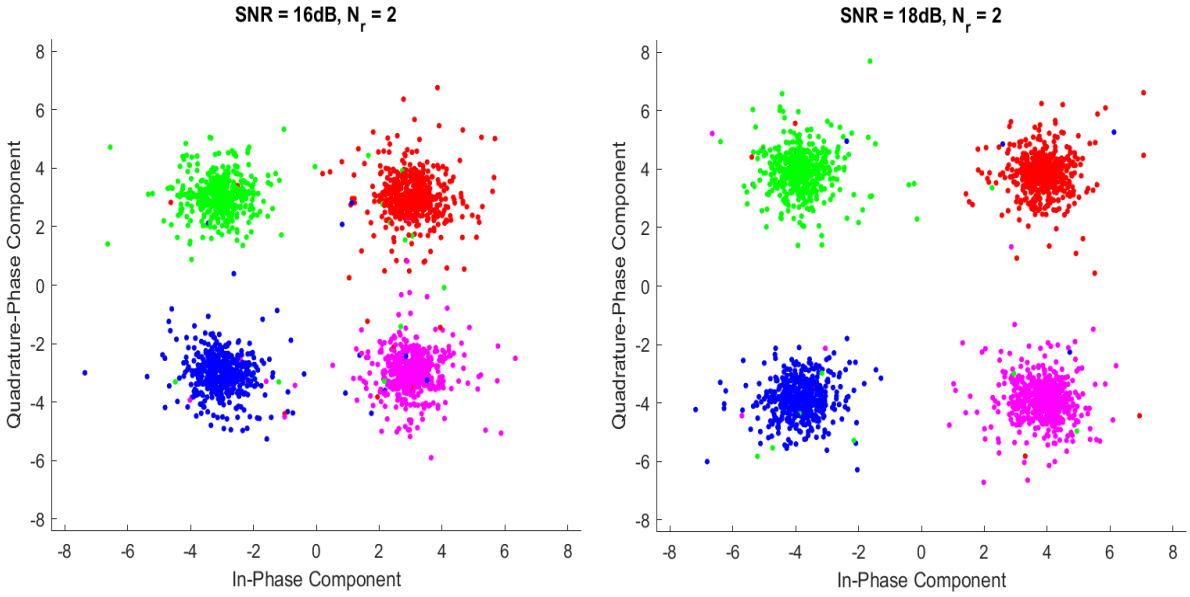

Figure 6.8: SS-GSM Scatter plot of the projection of the received vector on the learned channel using CNN(Traditional ML) at SNR of 16dB and 18dB

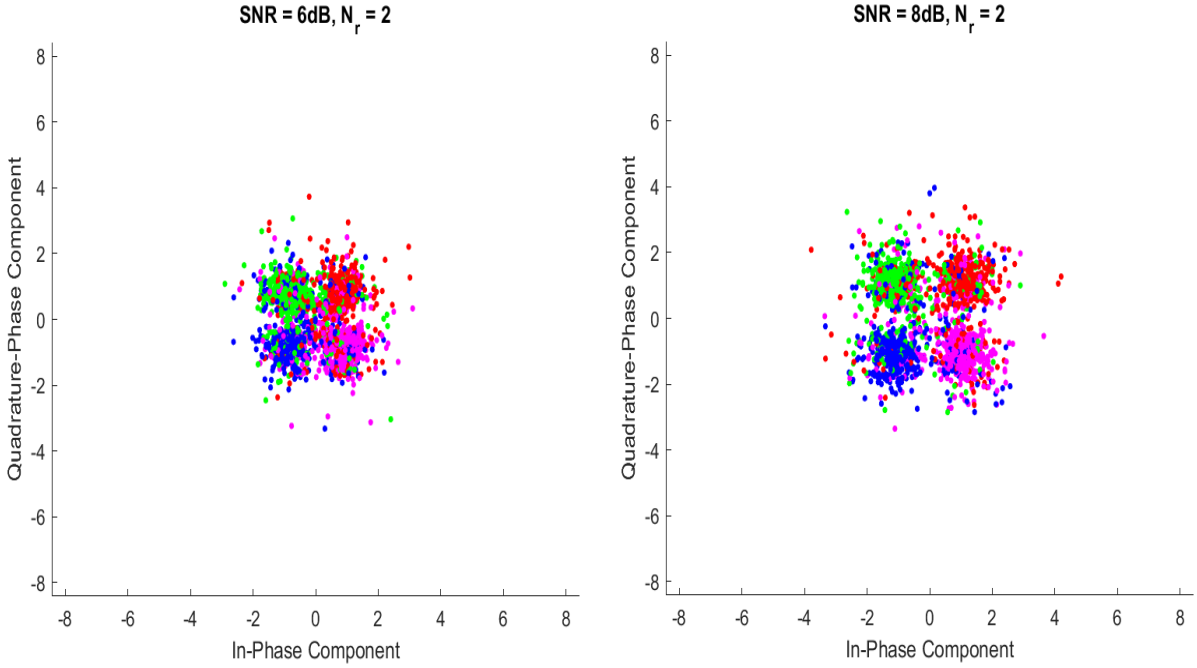

Figure 6.9: SS-GSM Scatter plot of the projection of the received vector on the learned channel using CNN(Proposed ML) at SNR of 6dB and 8dB

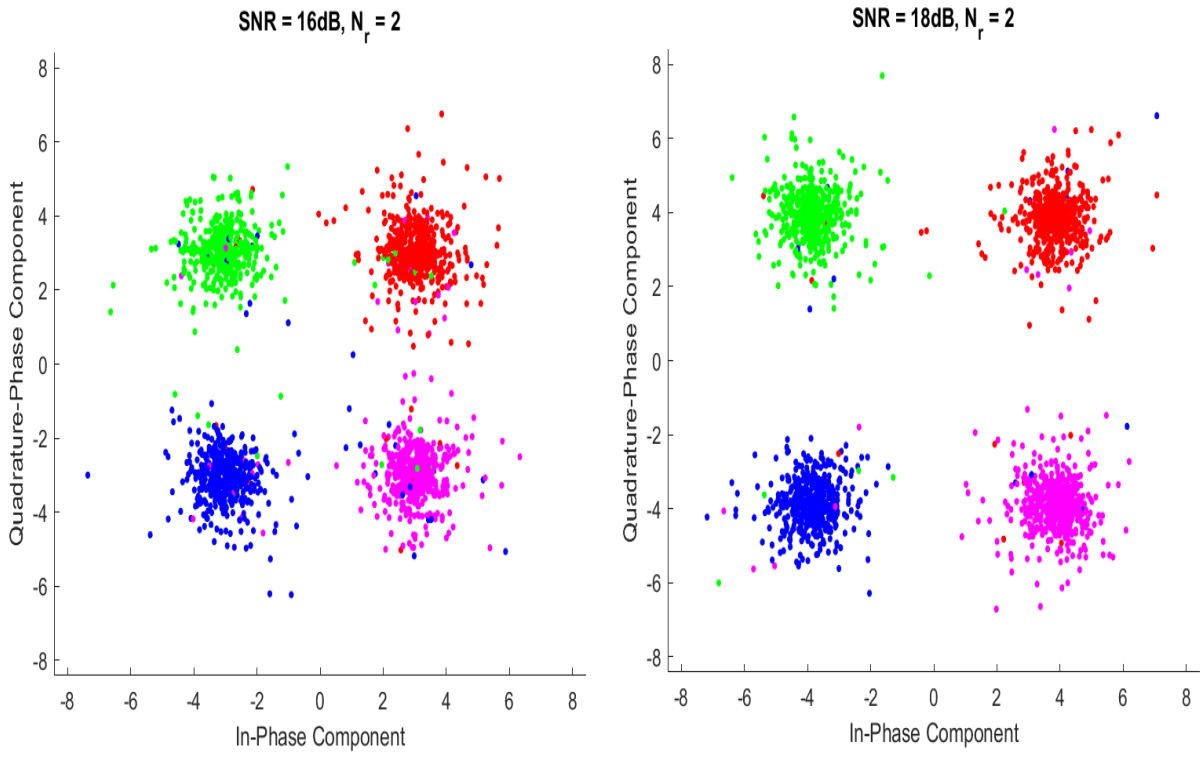

Figure 6.10: SS-GSM Scatter plot of the projection of the received vector on the learned channel using CNN(Proposed ML) at SNR of 16dB and 18dB

In the two proposed methods, as the transmission power is increased, the learned channel statues will produce separable classes which makes the detection process more accurate.

Confusion Matrices

The confusion matrix is applied separately on the detected spatial channel index and on the detected signal constellation index for the proposed CNN for the two cases: the traditional extracted features given by Eq. 5.4 and the proposed extracted features given by Eq. 5.7, and the results are as shown in figures 6.6 and 6.7. The confusion matrix is applied to the detected symbols instead of the detected bits. The system configuration is as follows: $N_r = 2$, $N_t = 5$, $N_a = 2$, $M = 4$, and $SNR = 16dB$ for the SS-GSM scheme.

The total average accuracies for the two AE-CV-CNN are very close to each other.

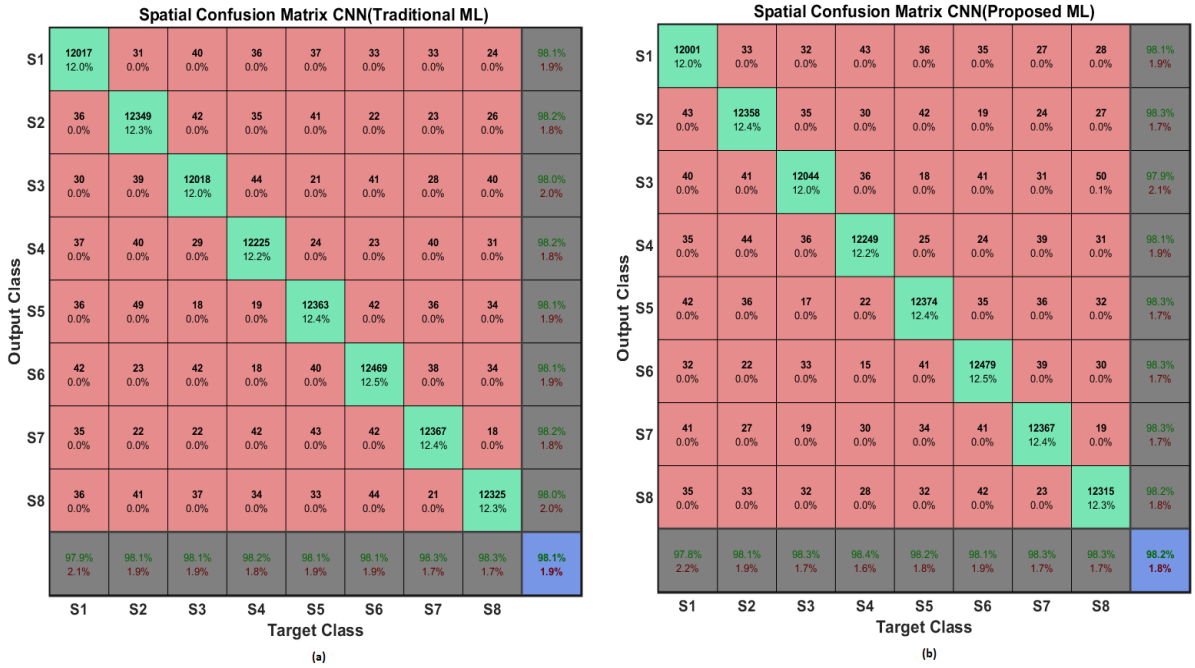

Figure 6.11: Confusion Matrices for the applied AE-CV-CNN: (a) Traditional ML extracted features, (b) Proposed ML extracted features.

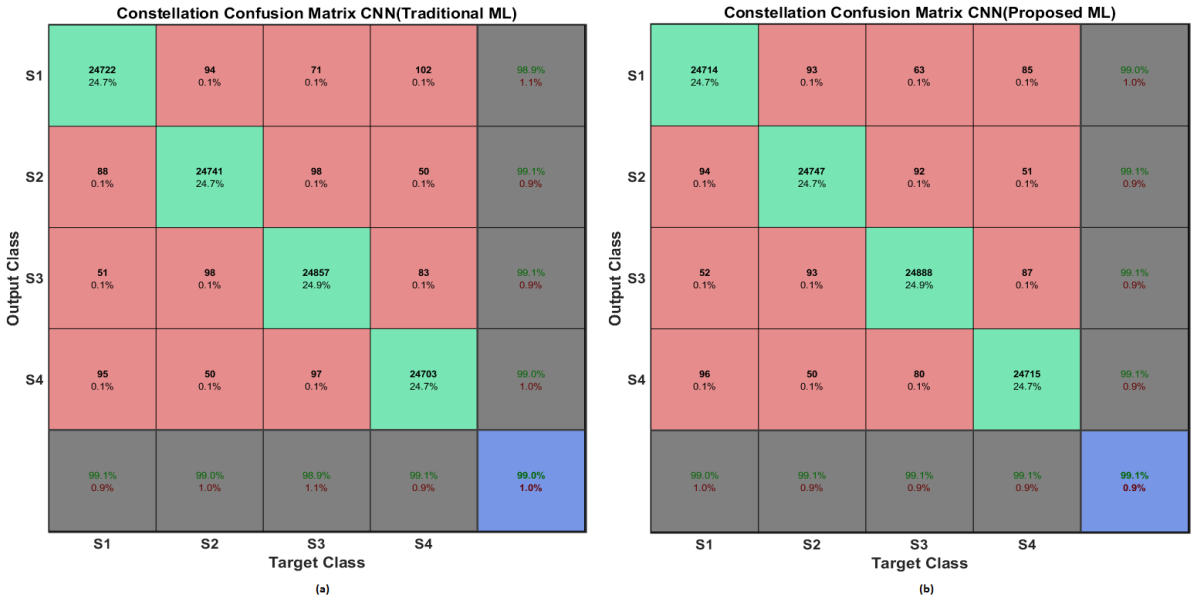

Figure 6.12: Confusion Matrices for the applied AE-CV-CNN: (a) Traditional ML extracted features, (b) Proposed ML extracted features.

6.2.2 MS-GSM system

Accuracy

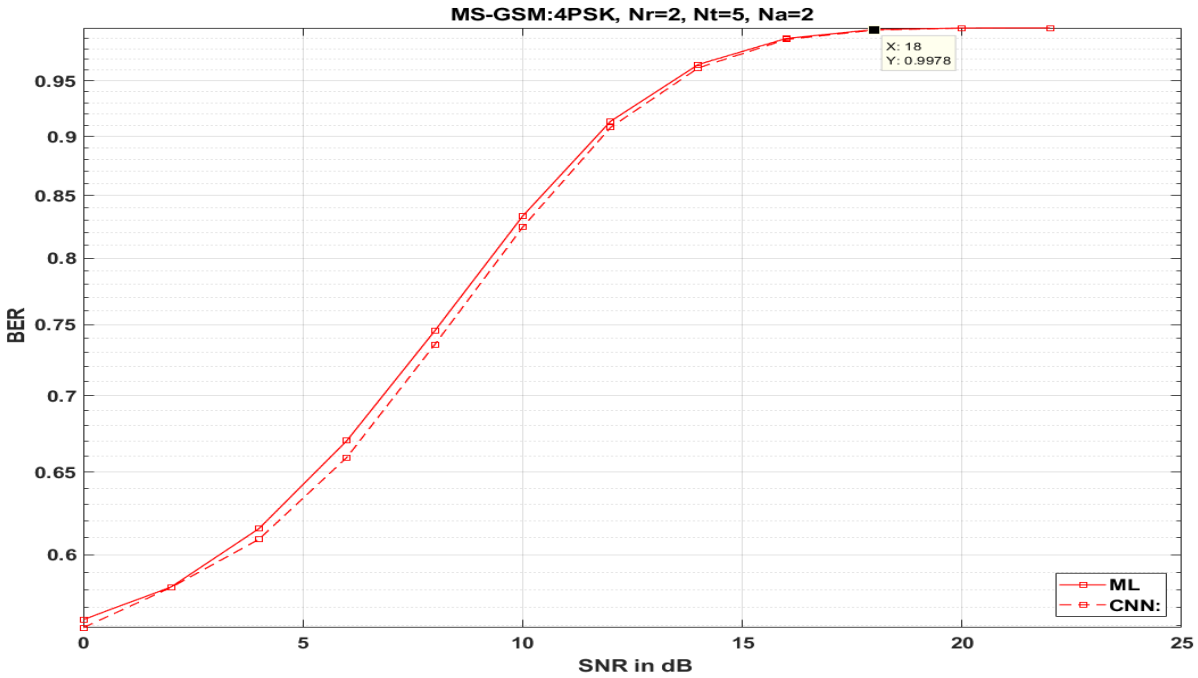

Figure 6.13: MS-GSM Confusion Matrix for the QPSK transmitted Symbols.

Bit Error Rate

Confusion Matrices

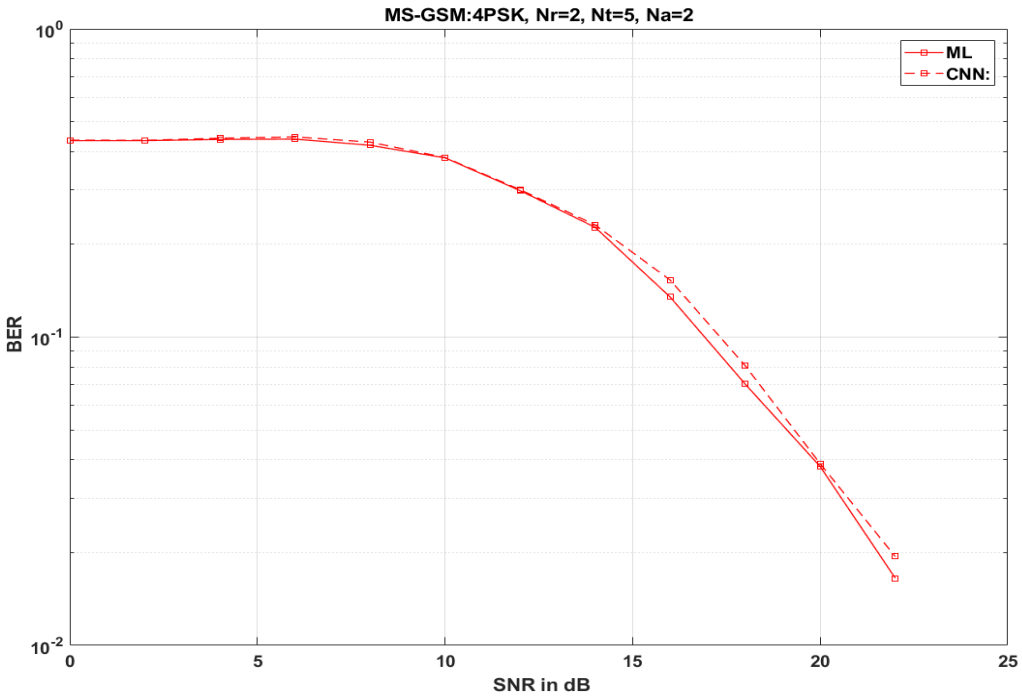

Figure 6.14: MS-GSM Bit Error Rate.

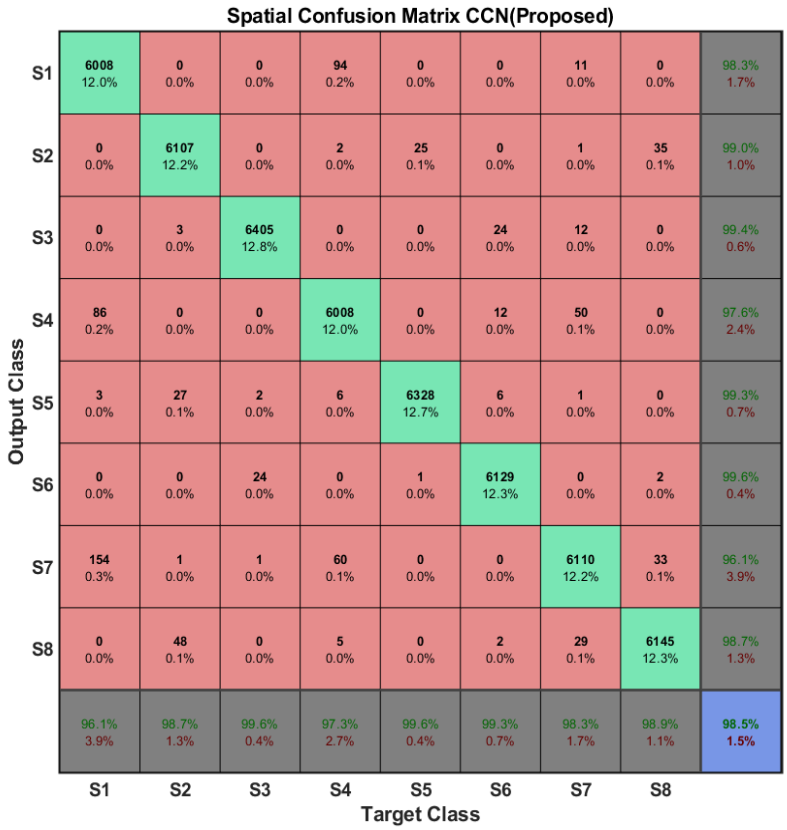

Figure 6.15: MS-GSM Spatial Confusion Matrices for the applied AE-CV-CNN.

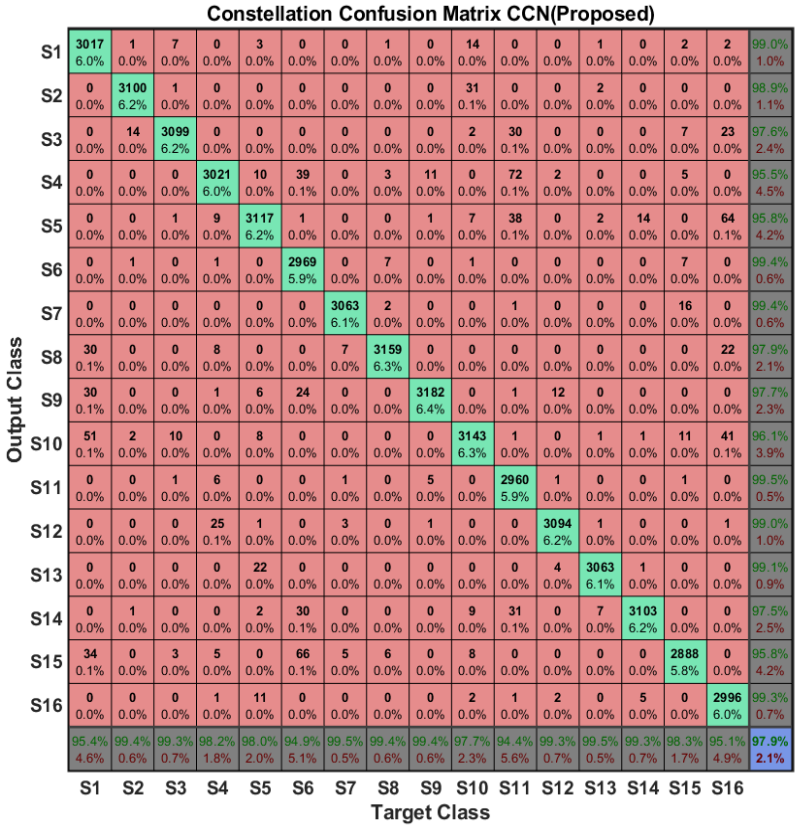

Figure 6.16: MS-GSM Modulation Confusion Matrices using AE-CV-CNN.

Chapter 7

Conclusion

The novel proposed auto-encoder complex valued convolutional neural network is applicable for the physical layer of MIMO wireless netowrks and achieves significant complexity reduction especially for single symbol generalized spatial schemes. The proposed model is tailored to reduce the computational complexity for the detection process which is a cost intensive on the existing detection algorithms. The minimum reduction of the computational complexity is 63.64% for single symbol generalization spatial modulation systems using $MPSK$ schemes. As a result, the power consumption at the receiver will be reduced which means increasing the energy efficiency. In terms of the spectrum energy, as the spectrum efficiency is increased, the **reduction** on the computational complexity with respect to the complexity of the maximum likelihood detector is increased. For example, for a spatial size of 8 the computational reduction is 70.45% while for the spatial size of 16, the computational reduction is 73.86%. With the use of spatial modulation, the spectrum efficiency in terms of the number of transmitted bits per second per Hertz is increased without increasing neither the transmission bandwidth nor the transmission power.

Chapter 8

Future Work

To reduce the latency of the delivered data, the proposed model can be used as a complete unsupervised machine learning without learning the channel coefficients. In other words, the proposed model can be used for differential non coherent detection where the channel status remains almost constant for a sequence of transmissions. In addition, the existing orthogonal frequency division multiplexing radio access technique can be implemented on top of the proposed model. Another possible implementation of the neural networks at the air interface is for the detection of the modulation scheme. This is will be useful in the case of using adaptive modulation schemes to increase the link robustness where the modulation order is decreased for low accuracy and increased for high accuracy.

Bibliography

[1] K. Xiao, F. Wang, H. Rutagemwa, K. Michel and B. Rong, “High-performance multicast services in 5G big data network with massive MIMO," 2017 IEEE International Conference on Communications (ICC), Paris, 2017, pp. 1-6.

[2] J. Akhtman and L. Hanzo, "Power Versus Bandwidth-Efficiency in Wireless Communications: The Economic Perspective," 2009 IEEE 70th Vehicular Technology Conference Fall, Anchorage, AK, 2009, pp. 1-5.

[3] R. I. Ansari et al., "5G D2D Networks: Techniques, Challenges, and Future Prospects," in IEEE Systems Journal,2017, vol. PP, no. 99, pp. 1-15.

[4] S. Yamaguchi, H. Nakamizo, S. Shinjo, K. Tsutsumi, T. Fukasawa and H. Miyashita, “Development of active phased array antenna for high SHF wideband massive MIMO in 5G," 2017 IEEE International Symposium on Antennas and Propagation & USNC/URSI National Radio Science Meeting, San Diego, CA, USA, 2017, pp. 1463-1464.

[5] R. Hussain, A. T. Alreshaid, S. K. Podilchak and M. S. Sharawi, "Compact 4G MIMO antenna integrated with a 5G array for current and future mobile handsets," in IET Microwaves, Antennas & Propagation, vol. 11, no. 2, pp. 271-279, 1 29 2017.

[6] S. Dixit and H. Katiyar, "Performance of OFDM in Time Selective Multipath

Fading Channel in 4G Systems," 2015 Fifth International Conference on Communication Systems and Network Technologies, Gwalior, 2015, pp. 421-424. doi: 10.1109/CSNT.2015.107.

[7] Q. Ma et al., "Power Allocation for OFDM with Index Modulation," 2017 IEEE 85th Vehicular Technology Conference (VTC Spring), Sydney, NSW, 2017, pp. 1-5.

[8] M. Agiwal, A. Roy and N. Saxena, "Next Generation 5G Wireless Networks: A Comprehensive Survey," in IEEE Communications Surveys & Tutorials, vol. 18, no. 3, pp. 1617-1655, thirdquarter 2016.

[9] H. Q. Ngo, E. G. Larsson and T. L. Marzetta, "Energy and Spectral Efficiency of Very Large Multiuser MIMO Systems," in IEEE Transactions on Communications, vol. 61, no. 4, pp. 1436-1449, April 2013.

[10] D. Feng, C. Jiang, G. Lim, L. J. Cimini, G. Feng and G. Y. Li, "A survey of energy-efficient wireless communications," in IEEE Communications Surveys & Tutorials, vol. 15, no. 1, pp. 167-178, First Quarter 2013.

[11] B. Zheng, M. Wen, E. Basar and F. Chen, "Low-complexity near-optimal detector for multiple-input multiple-output OFDM with index modulation," 2017 IEEE International Conference on Communications (ICC), Paris, 2017, pp. 1-6.

[12] B. Zheng, M. Wen, E. Basar and F. Chen, "Multiple-Input Multiple-Output OFDM With Index Modulation: Low-Complexity Detector Design," in IEEE Transactions on Signal Processing, vol. 65, no. 11, pp. 2758-2772, June1, 1 2017.

[13] A. Younis, N. Serafimovski, R. Mesleh and H. Haas, “Generalised spatial modulation," 2010 Conference Record of the Forty Fourth Asilomar Conference on Signals, Systems and Computers, Pacific Grove, CA, 2010, pp. 1498-1502.

[14] C. T. Lin, W. R. Wu and C. Y. Liu, "Low-Complexity ML Detectors for Generalized Spatial Modulation Systems," in IEEE Transactions on Communications, vol. 63, no. 11, pp. 4214-4230, Nov. 2015.

[15] T. OâĂŹShea and J. Hoydis, "An Introduction to Deep Learning for the Physical Layer," in IEEE Transactions on Cognitive Communications and Networking, vol. 3, no. 4, pp. 563-575, Dec. 2017.

[16] J. Proakis, “Deterministic and Random Signal Analysis,” in Digital Communications 4th ed. NY, McGraw-Hill, 2001, ch. 4, pp 165.

[17] J. Li, M. Wen, X. Cheng, Y. Yan, S. Song and M. H. Lee, "Differential Spatial Modulation With Gray Coded Antenna Activation Order," in IEEE Communications Letters, vol. 20, no. 6, pp. 1100-1103, June 2016.

[18] M. Ding, P. Wang, D. LÃşpez-PÃl’rez, G. Mao and Z. Lin, "Performance Impact of LoS and NLoS Transmissions in Dense Cellular Networks," in IEEE Transactions on Wireless Communications, vol. 15, no. 3, pp. 2365-2380, March 2016.

[19] T. Tuovinen, N. Tervo and A. PÃd’rssinen, "Downlink output power requirements with an experimental-based indoor LOS/NLOS MIMO channel models at 10 GHz to provide 10 Gbit/s," 2016, 46th European Microwave Conference (EuMC), London, 2016, pp. 505-508.

[20] Andreas F. Molisch, "Statistical Description of the Wireless Channel," in Wireless Communications , 1, Wiley-IEEE Press, 2011, 69-99.

[21] http://www.dsplog.com/2008/07/14/rayleigh-multipath-channel/

[22] Yoshihiko Akaiwa, "Other Topics in Digital Mobile Radio Transmission," in Introduction to Digital Mobile Communication , 1, Wiley Telecom, 2015, pp.375-401.

[23] S. Afridi and S. A. Hassan, “Spectrally efficient adaptive generalized spatial modulation MIMO systems,“ 2017 $14th$ IEEE Annual Consumer Communications & Networking Conference (CCNC), Las Vegas, NV, 2017, pp. 260-263.

[24] M. Di Renzo, H. Haas, A. Ghrayeb, S. Sugiura and L. Hanzo, “Spatial Modulation for Generalized MIMO: Challenges, Opportunities, and Implementation,“ in Proceedings of the IEEE, vol. 102, no. 1, pp. 56-103, Jan. 2014.

[25] Houman Zarrinkoub, “Overview of the LTE Physical Layer”, in Understanding LTE with MATLAB:From Mathematical Modeling to Simulation and Prototyping, John Wiley & Sons, Ltd, 2014, pp 13-46.

[26] R. Mesleh, H. Haas, C. W. Ahn and S. Yun, "Spatial Modulation - A New Low Complexity Spectral Efficiency Enhancing Technique," 2006 First International Conference on Communications and Networking in China, Beijing, 2006, pp. 1-5.

[27] R. Y. Mesleh, H. Haas, S. Sinanovic, C. W. Ahn and S. Yun, "Spatial Modulation," in IEEE Transactions on Vehicular Technology, vol. 57, no. 4, pp. 2228-2241, July 2008.

[28] R. M. Legnain, R. H. M. Hafez, I. D. Marsland and A. M. Legnain, ”A novel spatial

modulation using MIMO spatial multiplexing," 2013 1st International Conference on Communications, Signal Processing, and their Applications (ICCSPA), Sharjah, 2013, pp. 1-4.

[29] S. DÃűrner, S. Cammerer, J. Hoydis and S. ten Brink, “Deep Learning-Based Communication Over the Air,” in IEEE Journal of Selected Topics in Signal Processing, vol. PP, no. 99, pp. 1-1.

[30] Y. Ding, X. Zhang and J. Tang, ‘Machine Learning Basics,” in Deep Learning, MIT Press, 2016.

[31] D. Michie, D.J. Spiegelhalter, and C.C. Taylor “Classification,” in Machine Learning, Neural and Statistical Classification, 1994, ch. 2, pp 14-24.

[32] S. O. Hykin, “Introduction,” in Neural Networks and Learning Machines 3th ed. NJ, Pearson Prentice Hall, 2009, ch. 1, pp 1-67.

[33] https://medium.com/@xenonstack/overview-of-artificial-neural-networks-and-its-applications-2525c1addff7.

[34] R. Aggarwal and Y. Song, "Artificial neural networks in power systems. I. General introduction to neural computing," in Power Engineering Journal, vol. 11, no. 3, pp. 129-134, June 1997.

[35] C. T. Lin, W. R. Wu and C. Y. Liu, "Low-Complexity ML Detectors for Generalized Spatial Modulation Systems," in IEEE Transactions on Communications, vol. 63, no. 11, pp. 4214-4230, Nov. 2015.

[36] https://www.mathworks.com/discovery/convolutional-neural-network.html

[37] J. Li, G. Liu, H. W. F. Yeung, J. Yin, Y. Y. Chung and X. Chen, "A novel stacked denoising autoencoder with swarm intelligence optimization for stock index prediction," 2017 International Joint Conference on Neural Networks (IJCNN), Anchorage, AK, 2017, pp. 1956-1961.

[38] Y. Ding, X. Zhang and J. Tang, "A noisy sparse convolution neural network based on stacked auto-encoders," 2017 IEEE International Conference on Systems, Man, and Cybernetics (SMC), Banff, AB, 2017, pp. 3457-3461.

[39] C. Jiang, H. Zhang, Y. Ren, Z. Han, K. C. Chen and L. Hanzo, "Machine Learning Paradigms for Next-Generation Wireless Networks," in IEEE Wireless Communications, vol. 24, no. 2, pp. 98-105, April 2017.

[40] T. J. OâĂŹShea, T. Erpek, and T. C. Clancy (2017),found as “arXiv:1707.07980v1 [cs.IT].”

[41] X. Yan, F. Long, J. Wang, N. Fu, W. Ou and B. Liu, "Signal detection of MIMO-OFDM system based on auto encoder and extreme learning machine," 2017 International Joint Conference on Neural Networks (IJCNN), Anchorage, AK, 2017, pp. 1602-1606.